JACS
JOURNAL OF THE AMERICAN CHEMICAL SOCIETY

ARTICLE

pubs.acs.org/JACS

Selectivity and Mechanism of Hydrogen Atom Transfer by an Isolable Imidoiron(III) Complex

Ryan E. Cowley,[†] Nathan A. Eckert,[†] Sridhar Vaddadi,[‡] Travis M. Figg,[‡] Thomas R. Cundari,*[,‡] and Patrick L. Holland*[,†]

[†]Department of Chemistry, University of Rochester, Rochester, New York, 14627, United States

[‡]Department of Chemistry and Center for Advanced Scientific Computing and Modeling, University of North Texas, Denton, Texas, 76203, United States

Supporting Information

ABSTRACT: In the literature, iron−oxo complexes have been isolated and their hydrogen atom transfer (HAT) reactions have been studied in detail. Iron−imido complexes have been isolated more recently, and the community needs experimental evaluations of the mechanism of HAT from late-metal imido species. We report a mechanistic study of HAT by an isolable iron(III) imido complex, L^{Me}FeNAd (L^{Me} = bulky β-diketiminate ligand, 2,4-bis(2,6-diisopropylphenylimido)pentyl; Ad = 1-adamantyl). HAT is preceded by binding of *tert*-butylpyridine (^{t}Bupy) to form a reactive four-coordinate intermediate L^{Me}Fe(NAd)(^{t}Bupy), as shown by equilibrium and kinetic studies. In the HAT step, very large substrate H/D kinetic isotope effects around 100 are consistent with C−H bond cleavage. The elementary HAT rate constant is increased by electron-donating groups on the pyridine additive, and by a more polar medium. When combined with the faster rate of HAT from indene versus cyclohexadiene, this trend is consistent with H^+ transfer character in the HAT transition state. The increase in HAT rate in the presence of ^{t}Bupy may be explained by a combination of electronic (weaker Fe=N π-bonding) and thermodynamic (more exothermic HAT) effects. Most importantly, HAT by these imido complexes has a strong dependence on the size of the hydrocarbon substrate. This selectivity comes from steric hindrance by the spectator ligands, a strategy that has promise for controlling the regioselectivity of these C−H bond activation reactions.

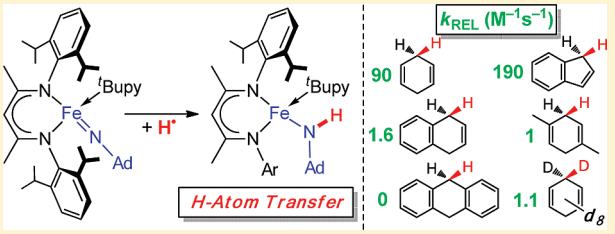

INTRODUCTION

Hydrogen atom transfer (HAT, eq 1) is an elementary chemical transformation that results in the net transfer of both a proton and an electron.[1,2] Metal−oxo complexes are widely used to abstract hydrogen atoms from organic compounds through HAT, which leads to the metal hydroxide (Scheme 1).[3] In oxidations by cytochrome P450, the mechanism is generally accepted to be HAT to an iron−oxo species (Fe=O) followed by radical rebound.[4] Other enzymatic systems such as soluble methane monooxygenase,[5] ribonucleotide reductases and other B_{12}-dependent enzymes,[6] lipoxygenases,[7] isopenicillin-*N* synthase,[8] and TauD[9] also utilize mechanisms with key HAT steps.

$$A{-}H + B^{\bullet} \rightarrow A^{\bullet} + B{-}H \qquad (1)$$

Considerable effort has been devoted to synthesizing and studying biomimetic oxoiron complexes[10] in order to help elucidate the enzymatic mechanisms and to develop homogeneous iron-based oxidation catalysts. Studies on heme iron−oxo complexes in the 1980s by Balch, La Mar, and Groves pioneered this field.[11] More recently, Que, Nam, and co-workers have reported isolable non-heme oxoiron(IV) complexes that react with hydrocarbons via HAT.[12] Reactions proceeding by HAT mechanisms have also been studied for terminal oxo complexes of Mn, Ru, Cr, and V.[13−19] In general, the selectivity of non-enzymatic HAT reactions is thermodynamically controlled, and reaction rates follow a linear correlation with the bond dissociation enthalpy (BDE) of the X−H bond being broken (the Bell−Evans−Polanyi relation),[1,20] i.e., homolytically weaker substrate bonds react more rapidly.

Imido (NR^{2-}) ligands are isoelectronic to oxo (O^{2-}) ligands (Scheme 1), and imido complexes are often proposed as intermediates in hydrocarbon amination mechanisms in which the imido species performs the cleavage of the C−H bond that precedes C−N bond formation. Imido complexes are also more versatile than oxo complexes, because there is an opportunity to tune the steric and electronic properties of the complex by changing the nitrogen substituent. However, the HAT reactivity of imido complexes (M=NR) has not been investigated in as much detail as that of their oxo counterparts. There has been a recent renaissance of activity in the synthesis of imido complexes of the late transition metals (groups 8−11),[21] and this activity has resulted in the isolation of late transition metal complexes

Received: January 18, 2011
Published: May 12, 2011

dx.doi.org/10.1021/ja2005303 | *J. Am. Chem. Soc.* 2011, 133, 9796–9811

Scheme 1. Analogy between HAT by Oxo and Imido Complexes

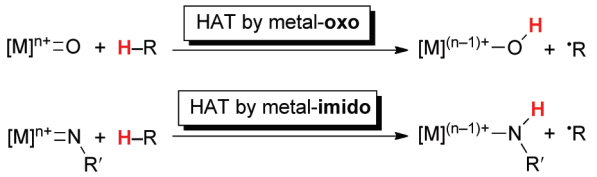

with terminal imido ligands for the first time.[22−27] Surprisingly, only a few of the *isolated* late-metal imido complexes perform HAT reactions, which has limited chemists' ability to evaluate the mechanism of HAT in imido systems. Warren' group demonstrated stoichiometric HAT with a nickel(III) imido complex,[27c] and Theopold's group showed that a Co−imido complex inserts the imide into a ligand C−H bond upon heating to form an amine complex.[25d] Betley's group has shown that an isolated iron−imido complex is capable of C−H amination, presumably through a HAT-based mechanism.[22m] Gallo's group reported an isolable Ru^{VI} diimido complex that catalyzes hydrocarbon amination through trappable radical intermediates.[23f] Che's group evaluated the effect of imido substituents and Ru(VI) reduction potential for imido transfer by a series of (porphyrinato)$Ru(NR)_2$ complexes.[23b]

In the chemistry of iron and other first-row metals, there are also reports of ligand C−H activation products that strongly implicate HAT by a reactive (but unobserved) imido moiety. For example, in 2003 Que's group observed ortho tosylamination of a ligand phenyl group upon addition of PhI=NTs to an iron(II) precursor and suggested an iron(IV) tosylimido intermediate.[28] More recently, the groups of Power,[22j] Warren,[29] Theopold,[30] Borovik,[31] Arnold,[32] Betley,[33] Peters,[34] and Latour[35] observed amido complexes of Fe, Co, or Cu whose formation is most easily rationalized as resulting from HAT by unobserved imido complexes. Stephan's group also observed radical reactivity of a putative Ni^{III} arylimido intermediate, in which radical attack at the para position of the arylimido moiety results in nickel−ketimido products.[36] In a few especially exciting cases,[29,33] ligand C−H activation leads to formation of a new N−C bond following the HAT step, likely through a "radical rebound" mechanism akin to the one used for hydroxylation by cytochrome P450.[4] However, the inability to isolate the presumed imido intermediates in these reactions prevented detailed study of the mechanisms.

We recently characterized the three-coordinate imidoiron(III) complex $L^{Me}Fe{=}NAd$ (**1**) (L^{Me} = 2,4-bis(2,6-diisopropylphenylimido)pentyl anion; Ad = 1-adamantyl) by EPR, NMR, and Mössbauer spectroscopies and density functional theory (DFT),[37] and subsequently by crystallography, EXAFS, and magnetic susceptibility.[38] It is especially notable that **1** brings about facile HAT reactions: our preliminary results suggested that the active species in HAT reactions was $L^{Me}Fe(NAd)(^tBupy)$ (**1**·^{t}**Bupy**) (^{t}Bupy = 4-*tert*-butylpyridine), which derives from weak coordination of **1** by added 4-*tert*-butylpyridine.[37] Because **1** is the first isolated iron−imido complex that performs intermolecular HAT reactions, it offers a special opportunity to gain insight into how these reactions proceed. In this study, we investigate the kinetics and thermodynamics of hydrocarbon HAT by **1**·^{t}**Bupy** using experimental and computational analysis. This is one of the first systematic studies of HAT reactivity of an isolated imido complex with any late transition metal.[23b,39] Iron-based imido complexes are especially exciting since there has been a surge in interest in the use of inexpensive and nontoxic iron for catalysis.[40]

Scheme 2. Intramolecular HAT by $L^{Me}FeNAd$ (1)

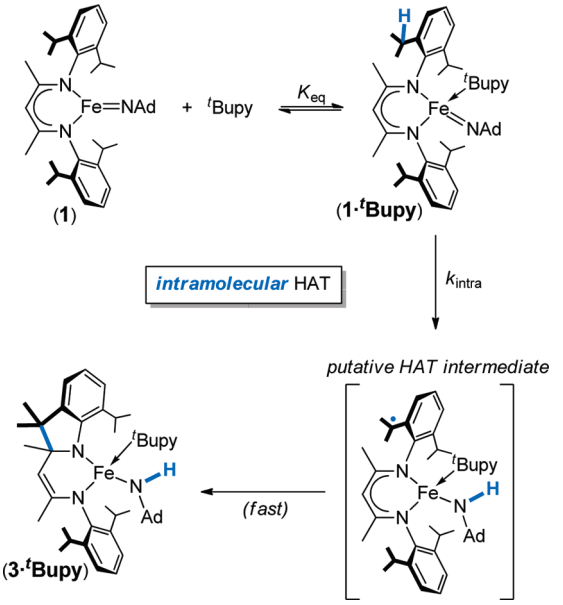

Scheme 3. Intermolecular HAT by $L^{Me}FeNAd$ (1)

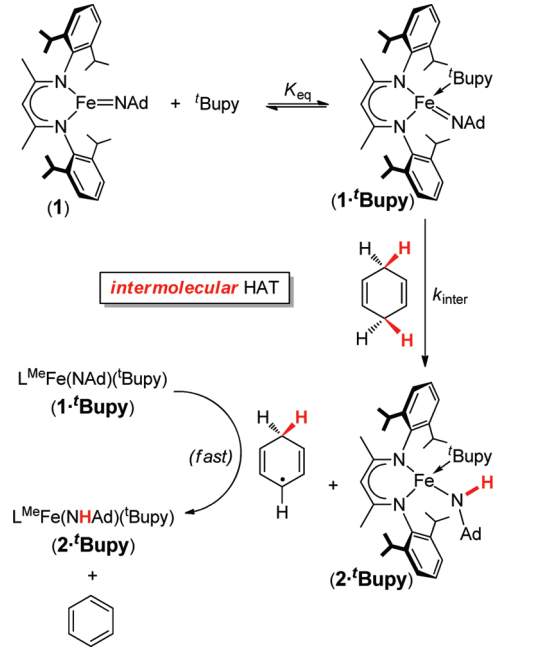

RESULTS

Hydrogen Atom Transfer Reactions of 1·^{t}Bupy. The imidoiron(III) complex $L^{Me}Fe{=}NAd$ (**1**) is produced upon addition of 2 equiv of N_3Ad to a THF solution of the formally diiron(I) dinitrogen complex $L^{Me}FeNNFeL^{Me}$.[38] In the presence of ^{t}Bupy, **1** exists in equilibrium with **1**·^{t}**Bupy** (see below).

dx.doi.org/10.1021/ja2005303 |*J. Am. Chem. Soc.* 2011, 133, 9796–9811

Table 1. Values of K_{eq} for Binding of Various Para-Substituted Pyridines to the Imido Complex 1[a]

pyridine substrate	T (°C)	K_{eq} (M^{-1})
4-^{t}Bupy	−51	250 ± 20
4-^{t}Bupy	−30	70 ± 7
4-^{t}Bupy	−15	27 ± 1
4-^{t}Bupy	0	15.4 ± 0.5
4-^{t}Bupy	25	4.4 ± 0.2
4-Me_2Npy	40	4.7 ± 0.3
4-^{t}Bupy	40	2.5 ± 0.1
4-Phpy	40	1.8 ± 0.1
4-F_3Cpy	40	0.8 ± 0.1

[a] Data obtained in C_7D_8 with [Fe] = 18 mM.

Although pyridine-free **1** is stable for several weeks at −45 °C, **1·^{t}Bupy** is significantly less stable and decomposes to the amidoiron(III) complex (L^{Me*})Fe(NHAd)(^{t}Bupy) (**3·^{t}Bupy**) within a few hours at room temperature.[37] In this reaction, the L^{Me} ligand undergoes intramolecular C−C coupling to form an asymmetric dianionic ligand (designated L^{Me*} here), presumably by way of HAT (Scheme 2). A solution of **1·^{t}Bupy** also rapidly reacts with 1,4-cyclohexadiene (CHD) to afford the amidoiron(II) complex L^{Me}Fe(NHAd)(^{t}Bupy) (**2·^{t}Bupy**) and benzene (Scheme 3).[37] Kinetic studies presented below are consistent with the mechanisms in Schemes 2 and 3.

Thermodynamics of Pyridine Coordination to 1. A necessary first step in the mechanistic inquiry is to quantify the equilibrium between **1** and **1·^{t}Bupy**. The equilibrium constants for binding of ^{t}Bupy to compound **1** were explored by evaluating the ^{1}H NMR signals of mixtures of **1** and ^{t}Bupy as a function of [^{t}Bupy]. Plotting the change in chemical shift versus $[^t\text{Bupy}]_0$ and fitting the data to a standard weak-binding equation[41] gave values for K_{eq} in the temperature range −51 to +40 °C (Table 1). The van't Hoff plot (Figure 1) gives values of ΔH_{eq}° = −7.0(2) kcal/mol and ΔS_{eq}° = −20.6(6) cal/mol·K, which are reasonable values for the proposed equilibrium: the exothermic ΔH_{eq}° value is consistent with a new bond being formed, and the negative ΔS_{eq}° value is consistent with combining two molecules into one. At 298 K, these values correspond to ΔG_{eq}° = −0.9(3) kcal/mol, a value that indicates very weak coordination. K_{eq} values for 4-phenylpyridine, 4-(dimethylamino)pyridine, and 4-(trifluoromethyl)pyridine were also determined at 40 °C. Table 1 shows that more electron-donating pyridines bind more strongly to **1**, as expected from their greater basicity.

Kinetic Studies of the Intramolecular HAT Reaction. The intramolecular hydrogen atom abstraction reaction (conversion of **1·^{t}Bupy** to **3·^{t}Bupy**, Scheme 2) was studied by ^{1}H NMR spectroscopy in C_6D_6 at 40 °C with [**1**] = 29 mM. The progress of the reaction was followed by monitoring the disappearance of **1** relative to a capillary integration standard.[42] The concentration of **1** decreased over time, and the relative integrations were fit to a first-order exponential curve[43] to obtain the observed pseudo-first-order rate constant k_{obs}. A plot of k_{obs} versus [^{t}Bupy] is shown in Figure 2. At low [^{t}Bupy], the observed rate has a near linear dependence on [^{t}Bupy], but the observed rate begins to saturate at [^{t}Bupy] ≈ 0.2 M. The observed saturation kinetics indicate a rapid pre-equilibrium involving ^{t}Bupy association prior to the rate determining step. The rapid equilibrium is consistent with the dynamic averaging of signals in the ^{1}H NMR spectrum of **1** and **1·^{t}Bupy**.

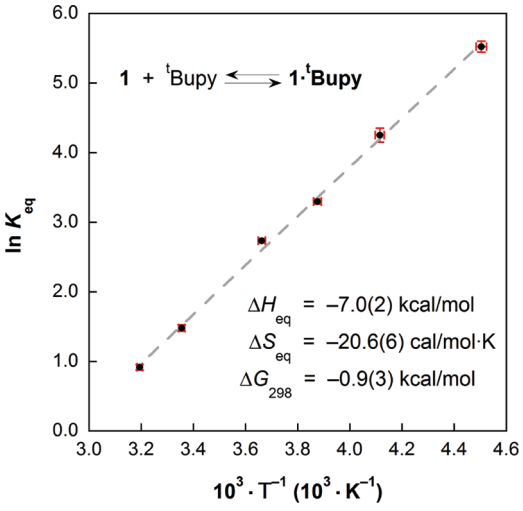

Figure 1. van't Hoff plot for ^{t}Bupy binding to **1** over a temperature range of −51(1) to +40(1) °C. Data obtained with [Fe] = 19 mM and [^{t}Bupy] = 0−0.53 M in toluene-d_8.

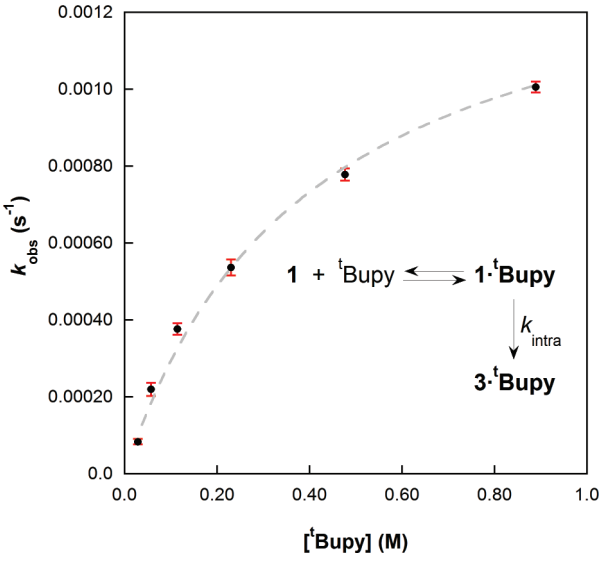

Figure 2. Observed rate of intramolecular HAT as a function of ^{t}Bupy concentration. Data obtained in C_6D_6 at 40(1) °C with [Fe] = 29 mM. The dashed line represents the fit to eq 3.

The intercept near the origin is consistent with the observation that decomposition of **1** proceeds at a greatly decreased rate at 40 °C without pyridine. When combined with the dependence of k_{obs} on [^{t}Bupy], this indicates that ***1·^{t}Bupy, and not 1, is the active species in the HAT reaction***. These data imply the rate law in eq 2, where k_{intra} is the first-order rate constant of the elementary HAT step.

$$-\frac{d[\mathbf{1}\cdot{}^t\mathbf{Bupy}]}{dt} = k_{intra}[\mathbf{1}\cdot{}^t\mathbf{Bupy}] \qquad (2)$$

Since ^{t}Bupy coordinates weakly to **1** at 40 °C (K_{eq} = 2.5(1) M^{-1}, see above), we can use the weak-binding approximation $[\mathbf{1}\cdot{}^t\mathbf{Bupy}]_{eq} \approx (K_{eq}[\mathbf{1}]_0[^t\text{Bupy}]_0)/(1 + K_{eq}[^t\text{Bupy}]_0)$ to obtain the rate law in eq 3, which expresses the rate in terms of the known

dx.doi.org/10.1021/ja2005303 |J. Am. Chem. Soc. 2011, 133, 9796–9811

parameters K_{eq}, $[\mathbf{1}]_0$, and $[^t\text{Bupy}]_0$.

$$-\frac{d[\mathbf{1}\cdot{}^t\mathbf{Bupy}]}{dt} = k_{intra}\left(\frac{K_{eq}[\mathbf{1}]_0[^t\text{Bupy}]_0}{\mathbf{1} + K_{eq}[^t\text{Bupy}]_0}\right) \quad (3)$$

By fitting eq 3 to the data in Figure 2, the elementary rate constant is calculated to be $k_{intra} = 5.1(1) \times 10^{-2}$ s^{-1} for the reaction of **1** and ^{t}Bupy. The pseudo-first-order rate constants k_{obs} were also determined using several para-substituted pyridines (40 °C, [Fe] = 26 mM, [pyridine] = 0.26 M). Assuming that the rate law in eq 3 applies to each reaction, it is possible to calculate the rate constants k_{intra} for the HAT reaction using each para-substituted pyridine (Table 2), using the independently determined values of K_{eq} (Table 1). The Hammett plot of the elementary rate constant k_{intra} as a function of σ_p shows that more electron-donating pyridine substituents (Figure 3) lead to faster HAT,[44] with a ρ value of −0.77(4).

Table 2. Pyridine Substituent Effects on the Intramolecular HAT Rate Constant[a]

pyridine para-substituent	k_{intra} (s^{-1}) at 40 °C
NMe_2	$1.5(2) \times 10^{-1}$
^{t}Bu	$5.1(1) \times 10^{-2}$
Ph	$3.1(2) \times 10^{-2}$
CF_3	$1.3(2) \times 10^{-2}$

[a] Data obtained at 40(1) °C in C_6D_6 with [**1**] = 77 mM and [pyridine] = 0−0.80 mM.

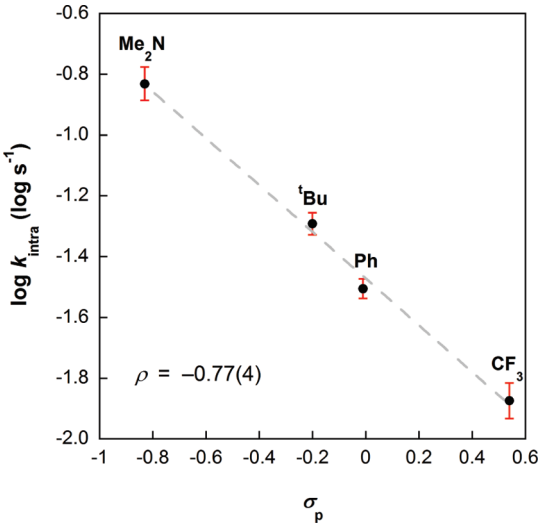

Figure 3. Hammett plot of para-substituted pyridines for the intramolecular HAT reaction (ref 44). Data obtained at 40(1) °C in C_7D_8. The slope of the dashed line gives $\rho = -0.77(4)$.

Intermolecular HAT Reaction with 1,4-Cyclohexadiene. Addition of certain reagents with weak C−H bonds such as CHD prevented intramolecular attack on the diketiminate ligand, in favor of an intermolecular reaction. For example, the product of reaction between **1**·^{t}**Bupy** and CHD was L^{Me}Fe(NHAd)(^{t}Bupy) (**2**·^{t}**Bupy**), observed in 91% yield by ^{1}H NMR spectroscopy. Hydrocarbons with stronger C−H bonds (e.g., toluene, with a benzylic C−H BDE ~89 kcal/mol[45]) did not react with **1**·^{t}**Bupy** prior to intramolecular HAT reaction. Therefore, the intermolecular HAT reactivity of **1**·^{t}**Bupy** is limited to substrates that react more quickly than the intramolecular reaction.

The rate of the reaction of **1**·^{t}**Bupy** with CHD was chosen for detailed kinetic study by ^{1}H NMR spectroscopy. The intermolecular reaction with CHD is much faster than the intramolecular HAT reaction discussed above, so the kinetic experiments were performed at −51(1) °C, a temperature at which the intramolecular HAT reaction is not observed. The disappearance of **1**·^{t}**Bupy** and concomitant appearance of **2**·^{t}**Bupy** were monitored by integration against a capillary integration standard.[42] In each case, the spectroscopically observed yield of **2**·^{t}**Bupy** was ≥90%. Under pseudo-first-order conditions ([**1**] = 51 mM, [^{t}Bupy] = 257 mM) at −51(1) °C in toluene-d_8, the reaction rate had a linear dependence on [CHD] between 0.13 and 0.79 M (Figure 4a), suggesting that the rate-limiting step is attack on the hydrocarbon. Similar to the intramolecular reaction, the intermolecular HAT rate is dependent on the presence of ^{t}Bupy. If ^{t}Bupy was omitted, no reaction was observed in 3 h at −51 °C (<5% decrease of the integration of **1**, and no **2** was detected). Since ^{t}Bupy binds more strongly at −50 °C ($K_{eq} = 250 \pm 20$ M^{-1}) than at 40 °C ($K_{eq} = 2.5 \pm 0.1$ M^{-1}), the rate of reaction with CHD saturates at a lower concentration of [^{t}Bupy] (Figure 4b) than the intramolecular HAT reaction. As with the intramolecular HAT reaction, the

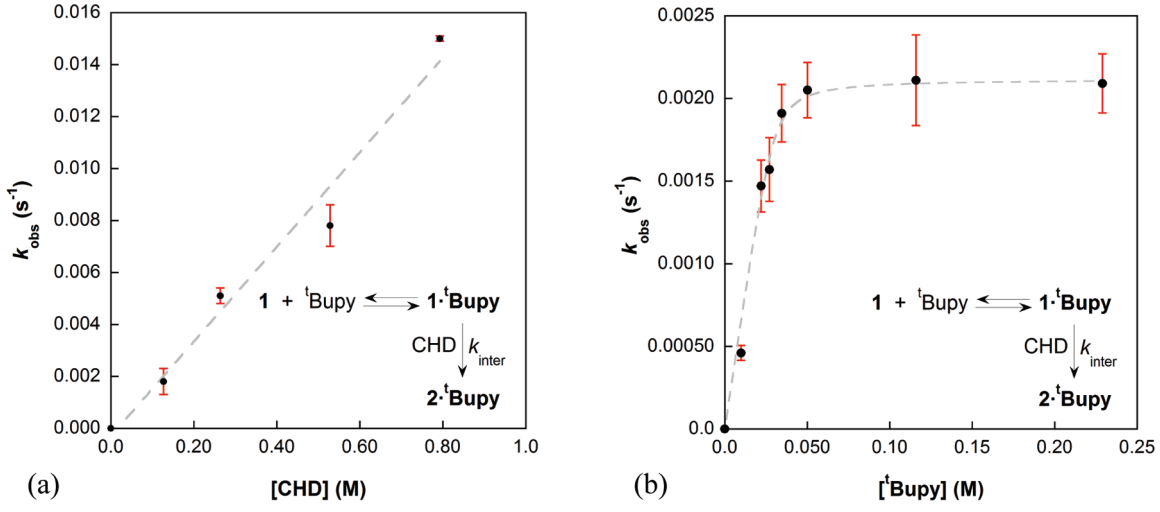

Figure 4. Observed rate of intermolecular HAT as a function of (a) 1,4-cyclohexadiene (CHD) concentration at constant [^{t}Bupy] = 257 mM and (b) ^{t}Bupy concentration at constant [CHD] = 150 mM. Data obtained in toluene-d_8 at −51(1) °C. The dashed line in panel b represents the fit to eq 5.

dx.doi.org/10.1021/ja2005303 |J. Am. Chem. Soc. 2011, 133, 9796–9811

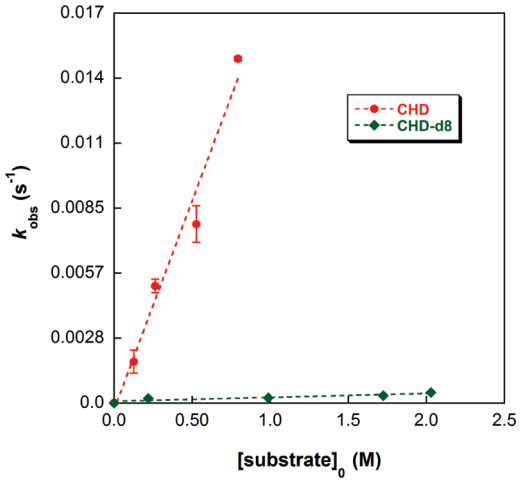

Figure 5. Comparison of observed rate constants for the intermolecular HAT reaction of **1**·^{t}**Bupy** with CHD and CHD-d_8. The ratio of slopes is 105 ± 28. Data obtained in toluene-d_8 at −51(1) °C with 51 mM Fe and 0.26 M ^{t}Bupy (for CHD) or 25 mM Fe and 0.20 M ^{t}Bupy (for CHD-d_8).

necessity for ^{t}Bupy implicates **1**·^{t}**Bupy** as the reactive form of the imido complex.

With the first-order dependence on [CHD], one expects the rate law in eq 4, where k_{inter} is the second-order rate constant for the elementary HAT step. The factor of 2 is added because CHD contains two weak C−H bonds and thus requires 2 equiv of **1**·^{t}**Bupy** to form benzene. This analysis assumes that the second C−H bond reacts with a second molecule of **1**·^{t}**Bupy** much faster than the first HAT, which is reasonable because the C−H BDE of cyclohexadienyl radical (22 kcal/mol) is significantly lower than the C−H BDE in cyclohexadiene (77 kcal/mol).[46]

$$-\frac{d[\mathbf{1}\cdot{}^t\mathbf{Bupy}]}{dt} = 2k_{inter}[CHD][\mathbf{1}\cdot{}^t\mathbf{Bupy}] \quad (4)$$

Since the reaction was monitored at low temperature where K_{eq} for ^{t}Bupy association is large (K_{eq} = 250 ± 20 M^{-1}), the weak-binding approximation used to generate eq 3 cannot be used here. Thus, the full expression for [**1**·^{t}**Bupy**] in terms of K_{eq}, $[\mathbf{1}]_0$, and $[^t\text{Bupy}]_0$ must be used, which gives the rate law in eq 5.

$$-\frac{d[\mathbf{1}\cdot{}^t\mathbf{Bupy}]}{dt} = 2k_{inter}[CHD]\left\{\left[\left([\mathbf{1}]_0 + [^t\text{Bupy}]_0 + \frac{1}{K_{eq}}\right) - \left\{\left([\mathbf{1}]_0 + [^t\text{Bupy}]_0 + \frac{1}{K_{eq}}\right)^2 - 4[\mathbf{1}]_0[^t\text{Bupy}]_0\right\}^{1/2}\right]/2\right\} \quad (5)$$

However, the rate law is greatly simplified in the saturation regime ([^{t}Bupy] > 0.05 M), where there is a zeroth-order dependence on [^{t}Bupy] (eq 6).

$$-\frac{d[\mathbf{1}\cdot{}^t\mathbf{Bupy}]}{dt} = 2k_{inter}[CHD][\mathbf{1}]_0 \quad (6)$$

Under pseudo-first-order conditions (saturated in [^{t}Bupy] and with excess CHD), $k_{obs} = 2k_{inter}[CHD]$, and the elementary second-order rate constant for the HAT step (k_{inter} = (9.1 ± 0.9) × 10^{-3} M^{-1} s^{-1}) is calculated from the slope of Figure 4a.

H/D Kinetic Isotope Effect for the Reaction of 1·^{t}Bupy and CHD. To probe the hypothesis that the rate-limiting step of the mechanism is hydrogen atom transfer, we measured the intermolecular kinetic isotope effect (KIE) of the reaction with CHD by extending the kinetic study to CHD-d_8 (Figure 5). The ^{1}H NMR method was identical to that described above for CHD-h_8, although much higher concentrations of CHD-d_8 were necessary to speed up the reaction to a practical rate at −51 °C. The calculated value k_H/k_D = 105 ± 28 is a very large primary KIE, which clearly supports the contention that HAT from CHD is the rate-limiting step in the transformation.

HAT from Larger Substrates. To explore the substrate dependence of the HAT reactivity of **1**·^{t}**Bupy**, we chose a range of substrates with C−H bonds that are weak enough to react prior to intramolecular attack on the supporting ligand. The kinetics of the reactions of **1**·^{t}**Bupy** with indene, 1,4-dihydronaphthalene (DHN), 9,10-dihydroanthracene (DHA), 1,4-dimethyl-1,4-cyclohexadiene (Me_2CHD), and 1,2,4,5-tetramethyl-1,4-cyclohexadiene (Me_4CHD) were each measured in experiments analogous to those for CHD. No reaction was observed with either Me_4CHD or DHA at −51 °C with [Fe] = 30 mM and [substrate] = 1.2 M (<2% decrease in [**1**·^{t}**Bupy**] in 3 h). In each of the other cases, a linear correlation of k_{obs} with [substrate] was observed (Supporting Information Figures S-2−S-7). In each case, the reaction was performed with at least 0.2 M ^{t}Bupy to ensure saturation in [^{t}Bupy]. Thus, for the reactions with substituted cyclohexadienes, the rate law is identical to eq 6. For the reaction with indene, the rate law is given in eq 7, which follows eq 6, except the factor of 2 is omitted since each indene molecule supplies a single hydrogen atom.

$$-\frac{d[\mathbf{1}\cdot{}^t\mathbf{Bupy}]}{dt} = k_{inter}[\text{indene}][\mathbf{1}\cdot{}^t\mathbf{Bupy}] = k_{inter}[\text{indene}][\mathbf{1}]_0 \quad (7)$$

1,1,3-Trideuteroindene (indene-d_3) was also studied to obtain a KIE. Comparing the values of k_{obs} for the reactions with indene and indene-d_3 (Supporting Information Figure S-10) gives a KIE of k_H/k_D = 80 ± 12, similar to the KIE for the reaction of **1**·^{t}**Bupy** with CHD. The rate constants for the elementary HAT step (k_{inter}) for all substrates are summarized in Table 3. Conversion to the expected products benzene, *p*-xylene, and naphthalene was confirmed by GC/MS (92%, 99%, and 69%, respectively).[47]

Activation Parameters for Intermolecular HAT. The rate constants k_{intra} and k_{inter} (for the reaction with CHD) were determined over the temperature range of 10−50 °C, and it was possible to determine the activation parameters of the HAT step by plotting ln(k/T) versus $1/T$ (Eyring plot, Figure 6) and ln(k) versus $1/T$ (Arrhenius plot, Supporting Information Figure S-1). Activation parameters for the intramolecular HAT reaction from the diketiminate ligand are $\Delta H^{\ddagger}_{intra}$ = 14.6(5) kcal/mol, $\Delta S^{\ddagger}_{intra}$ = −18(2) cal/mol·K, ln(A_{intra}) = 22(1) s^{-1}, and $E_{a,intra}$ = 15.2(5) kcal/mol. Activation parameters for the intermolecular HAT from CHD are $\Delta H^{\ddagger}_{inter}$ = 14.4(8) kcal/mol, $\Delta S^{\ddagger}_{inter}$ = −9(3) cal/mol·K, ln(A_{inter}) = 26(1) M^{-1} s^{-1}, and $E_{a,inter}$ = 15.0(8) kcal/mol. At 298 K, the activation barriers are $\Delta G^{\ddagger}_{intra,298}$ = 20(1) kcal/mol and $\Delta G^{\ddagger}_{inter,298}$ = 15(2) kcal/mol, respectively.

Computations. To help understand the role of ^{t}Bupy in the HAT reactions of **1**·^{t}**Bupy**, and to understand the steric dependence of the reaction, computations were performed on the amido products (**2** and **2**·^{t}**Bupy**), imido starting materials (**1** and

dx.doi.org/10.1021/ja2005303 |*J. Am. Chem. Soc.* 2011, 133, 9796–9811

Table 3. Second-Order Rate Constants for Intermolecular HAT Reactions with 1·^{t}Bupy[d]

Substrate	k_{inter} ($M^{-1}·s^{-1}$) at –51 °C	k_{rel}[a]	homolytic BDE (kcal/mol)[b]	heterolytic BDE (kcal/mol)[b]
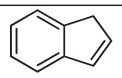	$(1.9 \pm 0.2) \times 10^{-2}$	190	77	351
	$(9.1 \pm 0.9) \times 10^{-3}$	90	71	375
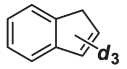	$(2.4 \pm 0.2) \times 10^{-4}$	2.4	–	–
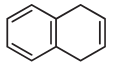	$(1.56 \pm 0.04) \times 10^{-4}$	1.6	72	366
	$(1.1 \pm 0.1) \times 10^{-4}$	1.1	–	–
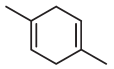	$(1.00 \pm 0.05) \times 10^{-4}$	1	71	376
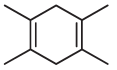	0[c]	0	71	375
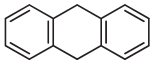	0[c]	0	74	359

[a] Second-order rate constant relative to the slowest measurable substrate (dimethyl-CHD). [b] Calculated for the allylic C–H bond at B3LYP/6-311++G(d,p) level of theory (see text). [c] With these substrates, even a high concentration of added substrate showed no intermolecular reaction at −51 °C (see text). We can place an upper limit on k_{inter} for these reactions at about 10^{-7} M^{-1} s^{-1}. [d] Kinetic data obtained in toluene-d_8 at −51(1) °C with [^{t}Bupy] = 0.26–0.52 M and [Fe] = 30–51 mM.

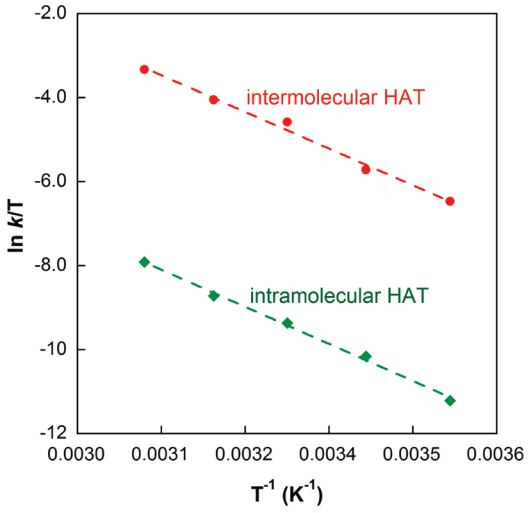

Figure 6. Eyring plots for intramolecular HAT (green diamonds) and intermolecular HAT from CHD (red circles) measured from 10 to 50 °C. The corresponding Arrhenius plots are given in Supporting Information Figure S-1.

1·^{t}Bupy), and transition states. Computations used a mixed quantum mechanical/molecular mechanics (QM/MM) model: B3LYP/6-311++G(d,p) on the N_2C_3Fe diketiminate core, the NC of the imido, and the pyridine ring, and UFF molecular mechanics[48] on the remainder of the complexes. We performed initial computations using a truncated model L′Fe(=NAd) (L′ = $C_3H_5N_2^-$) and the B3LYP/6-31G(d) functional/basis set to identify low-energy states for further study. The truncated models showed that in all imido ground states and transition states, the energies of the doublet spin states were much higher than those of the other spin states (≥10 kcal/mol), and so only quartets and sextets were considered in full QM/MM models. Moreover, tests with different functionals (BP86, M06, B2LYP, and MPWPW91) did not qualitatively alter the nature of the calculated potential energy curves.

Computations: Iron(III) Imido Complexes. The QM/MM methods were first validated on the crystallographically characterized three-coordinate complex **1**. The intermediate-spin state (Figure 7a) was computed to be 12 kcal/mol more stable (ΔH) than the high-spin isomer, which is in agreement with the $S = 3/2$ ground state identified by magnetometry and EPR spectroscopy.[38] The calculated bond distances and angles differ between the $S = 3/2$ and $S = 5/2$ states, and the corresponding bond distances and angles from the crystal structure of **1**[38] agree with the computed $S = 3/2$ geometry (Table 4), further supporting its intermediate spin-state assignment. In particular, the Y-shaped geometry at Fe and the short Fe–$N_{diketiminate}$ and Fe=N_{imido} distances of the crystal structure are reproduced well in the $S = 3/2$ model. A literature DFT model of the similar compound L^{xyl}Fe=NMe (L^{xyl} = 2,4-bis(2,6-dimethylphenylimido)pentyl) also predicted a spin-state dependence in the Fe=N bond length (1.68 Å for $S = 3/2$; 1.75 for $S = 5/2$).[49]

For the purposes of studying the HAT reactions, the four-coordinate pyridine adducts are also important. Enthalpy computations indicate that 1·^{t}Bupy is 2.4 kcal/mol more stable as a quartet (IS) than a sextet (HS). Inclusion of entropic factors yields a free energy difference in the HS and IS states of 1·^{t}Bupy

dx.doi.org/10.1021/ja2005303 |J. Am. Chem. Soc. 2011, 133, 9796–9811

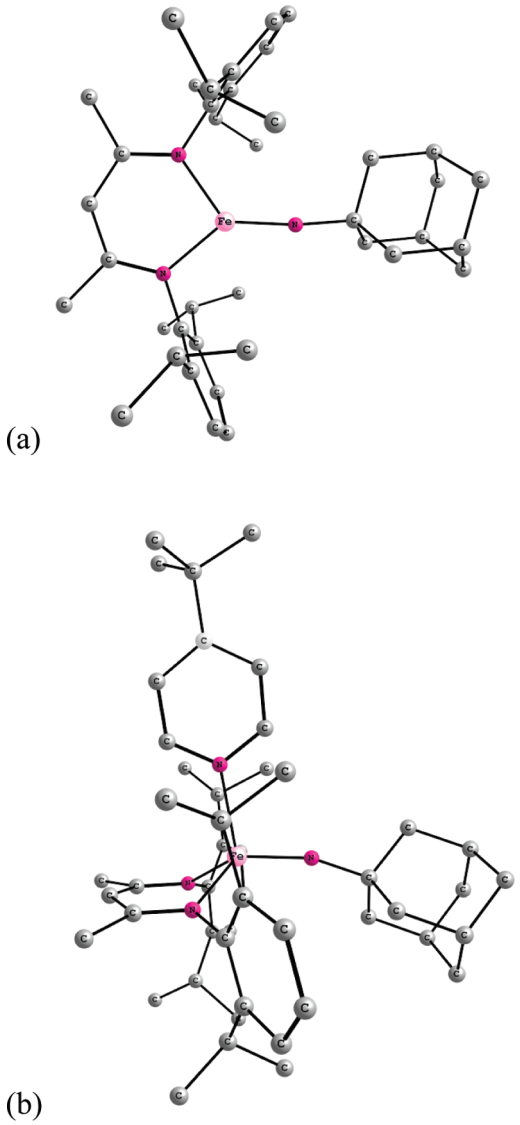

Figure 7. QM/MM-optimized geometries of (a) quartet **1** and (b) sextet **1·^{t}Bupy**. Hydrogen atoms are removed for clarity. Key: iron, light pink; nitrogen, dark pink; carbon, gray.

Table 4. Comparison of Bond Lengths and Angles between the Crystal Structure of 1 and the QM/MM-Optimized Geometries for S = 3/2 and S = 5/2 Spin States

	S = 3/2 model	S = 5/2 model	crystal structure[a]
Fe═N_{imido} (Å)	1.70	1.75	1.670(2)
Fe−$N_{diket.}$ (Å)	1.93; 1.94	1.99; 2.03	1.928(1); 1.918(1)
N_{diket}−Fe═N_{imido} (deg)	137; 127	157; 109	139.16(6); 126.82(6)
Fe═N_{imido}−C (deg)	173	163	170.40(13)
$N_{diket.}$−Fe−$N_{diket.}$ (deg)	95.6	94.1	94.02(6)

[a] Ref 38.

of only 0.2 kcal/mol, slightly in favor of the quartet. Because these are close to the same energy, both must be considered as potential ground-state candidates.[50] The optimized HS model of **1·^{t}Bupy** is shown in Figure 7b, and the optimized IS model is geometrically similar. Both spin states of **1·^{t}Bupy** have an iron coordination geometry that is distorted toward trigonal pyramidal.[51] The metrical parameters are given in Table 5. It is notable that regardless of spin state, the Fe═N bonds are significantly longer in the four-coordinate imido models (1.76 and 1.77 Å) than the quartet three-coordinate imido model (1.70 Å). These metrical parameters reflect weaker iron−nitrogen π-bonding in the four-coordinate species.

Table 5. Bond Lengths and Angles of the QM/MM-Optimized Geometries for S = 3/2 and S = 5/2 Spin States of 1·^{t}Bupy

	S = 3/2 model	S = 5/2 model
Fe═N_{imido} (Å)	1.76	1.77
Fe−N_{diket} (Å)	2.00; 2.01	2.07; 2.07
Fe−N_{py} (Å)	2.26	2.21
N_{diket}−Fe═N_{imido} (deg)	119; 138	118; 126
Fe═N_{imido}−C (deg)	169	162
N_{diket}−Fe−N_{diket} (deg)	95.7	90.2
N_{diket}−Fe−N_{py} (deg)	94.5; 100	109; 111
N_{py}−Fe═N_{imido} (deg)	100	102

Spin density was observed on the imido nitrogen in each complex. The nitrogen spin density is much greater in the S = 5/2 states (1.08 e$^-$ for **1·^{t}Bupy**; 1.07 e$^-$ for **1**) than in the S = 3/2 states (0.44 e$^-$ for **1·^{t}Bupy**; 0.26 e$^-$ for **1**). The spin localization on the imido ligand suggests that the sextet states of both **1** and **1·^{t}Bupy** may be alternatively described as iron(II) complexes with an imidyl radical anion ligands, (Fe^{2+})/($NAd^{\bullet-}$).[27c]

Computations: Iron(II) Amido Complexes and N−H Bond Enthalpies. The amido complexes **2** and **2·^{t}Bupy** were modeled with QM/MM methods in both triplet and quintet spin states. Geometry optimizations of amido complexes utilized the same QM/MM partitioning scheme applied to the full imido models, with the amido proton also modeled quantum mechanically. Smaller basis set QM/MM calculations (i.e., ONIOM(B3LYP/6-31+G(d):UFF)) indicated that the quintet amido product is more stable than the triplet amido product by 12 kcal/mol for **2** and by 18 kcal/mol for **2·^{t}Bupy**, which is consistent with their experimental room-temperature magnetic moments (~5.5 μ_B)[37,38] that suggest quintet ground states. Hence, simulations of **2** and **2·^{t}Bupy** with a larger QM basis set, ONIOM(B3LYP/6-311++G(d,p):UFF), were performed only on the quintet spin state.

The geometries of L^RFe−NHR′ have been found by crystallography to be quite sensitive to the particular amido (R′ = ^{t}Bu, Ph, tolyl, 2,6-Me_2Ph, 2,6-$i Pr_2$Ph) and β-diketiminate (R = Me, ^{t}Bu) substituents, as well as the presence or absence of a fourth ligand (THF, ^{t}Bupy),[52] which provides an opportunity to test the geometric predictions of the computations on **2** and **2·^{t}Bupy**. For the optimized structures of **2** and **2·^{t}Bupy**, there is asymmetry in the $N_{diket.}$−Fe−N_{amido} angles, large Fe−N_{amido}−C_{Ad} angles (~136−137°), and corresponding small Fe−N−H angles (~113°). Table 6 compares the calculated bond lengths and angles of **2** and **2·^{t}Bupy** to those determined experimentally from their crystal structures.[37,38]

The computed N−H homolytic BDEs are derived from the enthalpies of the amido and imido complexes and the calculated enthalpy of H$^\bullet$ (eq 8).

$$L^{Me}Fe(NAd)(^tBupy)_{0/1} + H^\bullet \rightarrow L^{Me}Fe(NHAd)(^tBupy)_{0/1} \quad (8)$$

dx.doi.org/10.1021/ja2005303 |J. Am. Chem. Soc. 2011, 133, 9796–9811

Table 6. Comparison of Calculated (QM/MM) and Experimental Bond Lengths and Angles for 2 and 2·^{t}Bupy

	$L^{Me}Fe(NHAd)$ (2)		$L^{Me}Fe(NHAd)(^tBupy)$ (2·^{t}Bupy)	
	QM/MM model	crystal structure[a]	QM/MM model	crystal structure[b]
$Fe-N_{amido}$ (Å)	1.88	1.860(2)	1.93	1.904(2)
$Fe-N_{diket.}$ (Å)	1.97; 1.99	1.974(2); 1.986(2)	2.06; 2.04	2.028(2); 2.030(2)
$Fe-N_{py}$ (Å)			2.23	2.171(2)
$N_{diket.}-Fe-N_{amido}$ (deg)	121; 145	121.04(8); 145.86(8)	120; 136	116.60(8); 137.13(8)
$N_{diket.}-Fe-N_{diket.}$ (deg)	94.4	93.09(3)	94.2	92.78(7)
$Fe-N_{amido}-C_{Ad}$ (deg)	136	134.7(2)	137	134.2(2)

[a] From ref 38(CSD refcode RUXBIW). [b] From ref 37 (CSD refcode XEPHEG).

For quintet **2**, the N−H homolytic BDE is calculated to be 89 kcal/mol relative to the quartet ground state of **1**. For quintet **2·^{t}Bupy**, the N−H bond enthalpy is calculated to be 85 kcal/mol relative to the sextet ground state of **1·^{t}Bupy**.

Computations: HAT Transition States. Transition states for C−H activation of CHD by **1** and by **1·^{t}Bupy** were evaluated with hybrid DFT/MM methods for both $S = 3/2$ and $S = 5/2$ spin states. Figure 8 depicts the quartet transition state for C−H activation of CHD by **1·^{t}Bupy**, which was slightly lower in enthalpy (6.4 kcal/mol) than the corresponding sextet transition state. In each transition state, the $Fe-N_{imido}$ bond has lengthened to 1.83−1.90 Å, and the Fe···N−C linkage has become more bent at 139−143°. The key three-center N···H···C interaction shows a similar geometry regardless of spin state or Fe coordination number, with a linear N···H···C angle (175−177°) and a slightly longer N···H (1.38−1.48 Å) distance than the C···H (1.23−1.33 Å) distance.

Interestingly, the barriers for HAT are calculated to be similar for the quartet and sextet transition states. So, even though sextet **1·^{t}Bupy** has greater spin density on the imido nitrogen atom *in the ground state* than quartet **1·^{t}Bupy**, it does not show a marked improvement in the kinetics of hydrogen atom abstraction. Additional evaluation of the barrier using other functionals and basis sets (BP86, M06, B2LYP, and MPWPW91 with the 6-311++G(d,p) basis set and B3LYP with 6-31+G(d) and the 6-311++G(d,p) basis sets) gave no clear preference, with the sign and magnitude of the relative quartet versus sextet barrier both being very sensitive to these details of the computation.

C−H Bond Dissociation Energies: Homolytic and Heterolytic. For a complete analysis of the HAT reaction, C−H BDEs for each substrate are needed. However, to our knowledge there are no literature values for the substituted cyclohexadienes used in the experiments above. Typically, there is only a small effect in the derived C−H BDE from peripheral substitution by hydrocarbyl groups, so the BDE values for methyl-substituted CHD are likely near the value for CHD. For example, xanthene (75.5) and 9-phenylxanthene (76.2) have nearly identical derived BDE values,[53] as do 9,10-dihydroanthracene (83.0) and 1,4,5,8-tetramethyl-9,10-dihydroanthracene (83.3).[54] Notwithstanding, multiple values for a single BDE are often encountered in the literature since various methods are used in their determinations.[55] Thus, we chose to calculate the BDE values for each substrate in this study using the B3LYP/6-311++G(d,p) level of theory (gas-phase simulations; enthalpies determined at 298.15 K and 1 atm) in order to have self-consistent and comparable numbers for all substrates. The computed C−H BDE values for each substrate are given in Table 3 above.

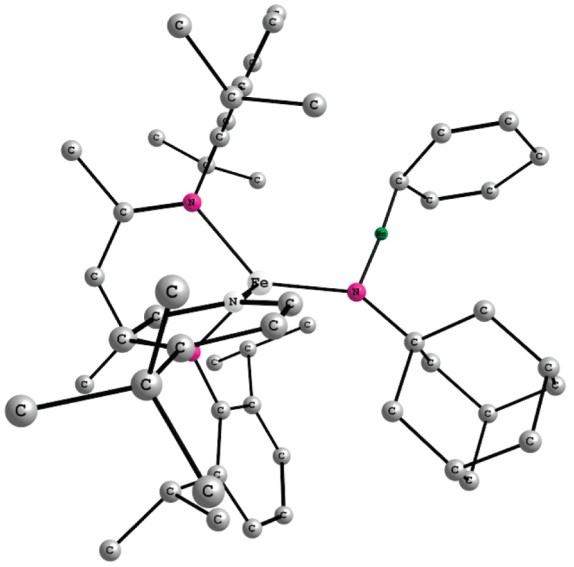

Figure 8. Quartet QM/MM-calculated transition state for C−H activation of CHD by **1·^{t}Bupy**.

We also sought the pK_a values for the substrates used in this study, especially to compare indene to the cyclohexadiene series. Empirical pK_a values are available for indene (20)[56] and DHA (30)[57] in DMSO, but the corresponding values for the substituted cyclohexadienes are, to our knowledge, unknown. Therefore, we computed the gas-phase enthalpy of heterolytic bond cleavage to give R^- and H^+ using the same B3LYP/6-311++G(d,p) level of theory employed for homolytic BDEs. The computed heterolytic C−H BDE values for each substrate are given alongside the homolytic BDEs in Table 3 above.

The calculated heterolytic BDEs are in excellent agreement with the available compiled enthalpic data.[58] The heterolytic BDE for 1,3-cyclohexadiene is given as 373.3 ± 4.1 kcal/mol,[59,60] which compares favorably with the calculated value of 375 kcal/mol for CHD. Two experimental evaluations of indene place its heterolytic BDE at 354.3 ± 2.5 kcal/mol[61] and 351.9 ± 2.1 kcal/mol,[62] both of which agree well with the B3LYP/6-311++G(d,p) value of 351 kcal/mol. Hence, the agreement between computations and the extant data is excellent with respect to both trends and magnitude.

DISCUSSION

Mechanism of C−H Activation by An Iron(III) Imido Complex. Iron(IV) oxo species have been established to abstract hydrogen

dx.doi.org/10.1021/ja2005303 |J. Am. Chem. Soc. 2011, 133, 9796–9811

atoms from hydrocarbons through HAT, which forms a new O−H bond and leaves an organic radical. The mechanisms of these reactions have been examined in detail in a number of important studies.[12] However, HAT by iron−imido complexes has not been studied because the few isolable iron−imido species are not capable of well-characterized intermolecular hydrogen atom abstraction reactions. In a few reported cases, additions of nitrene sources to iron(II) complexes have given iron(III) products that strongly imply HAT, but imido intermediates were not observed.[28,31,33,35] In contrast, the imidoiron(III) complex L^{Me}FeNAd (**1**) is isolable and characterized through crystallography, EXAFS, EPR, Mössbauer, NMR, computational chemistry, and magnetic susceptibility,[37,38] and in the presence of pyridines it reacts with hydrocarbons having weak C−H bonds. The study of **1** thus offers an excellent opportunity to learn more about the HAT ability of species with Fe=N bonds.

Interestingly, kinetic studies show that the HAT reactions of **1** take place almost exclusively through four-coordinate **1**·^{t}**Bupy**, as demonstrated by the dependence of the intramolecular reaction rate on the pyridine concentration. In the absence of pyridine, HAT requires significantly higher temperatures, and so our mechanistic investigations focused on the more rapid reaction of **1**·^{t}**Bupy**.

The mechanistic studies reported here provide strong evidence in support of a HAT mechanism for the reactions of **1**·^{t}**Bupy** with cyclohexadiene (CHD) and indene. The isolation and full characterization of the amidoiron products **2**·^{t}**Bupy** and **3**·^{t}**Bupy**[37] clearly show the net transfer of H$^\bullet$. In addition, the KIEs (KIE = ratio of rate constants with CHD/CHD-d_8 or indene/indene-d_3) are ≥80. Because this large KIE is greater than the classical limit of ∼7,[63] the reaction is likely to have a contribution from hydrogen tunneling.[64] The near-linear N···H···C angles in the calculated transition states are consistent with the opportunity for hydrogen tunneling. Very large H/D KIEs are a hallmark of HAT reactions.[65] For example, HAT from hydroquinone to *cis*-[Ru(bpy)$_2$(py)(O)]$^{2+}$ (bpy = 2,2′-bipyridine) shows k_{O-H}/k_{O-D} = 30,[66] and HAT from 9,10-dihydroanthracene to the octahedral iron(IV)−oxo complex (BPMCN)Fe^{IV}(O)(py) (BPMCN = *N*,*N*′-bis(2-pyridylmethyl)-*N*,*N*′-dimethyl-*trans*-1,2-diaminocyclohexane) shows k_{C-H}/k_{C-D} = 200.[12f] Values as large as k_H/k_D = 455 have been measured for a HAT reaction in an Os system.[67]

Trends in HAT Rate with Different Substrates. There is an extensive literature on HAT reaction rates, which have been measured for substrates having a wide range of C−H and O−H BDEs. In the 1960s, Ingold and co-workers studied HAT reactions of peroxy radicals with a large library of phenols and determined substituent effects on the second-order rate constants.[68] In a more recent example, Mayer and co-workers studied a range of different Fe, Co, and Ru systems that react with hydrocarbons or phenols via HAT[69] and found that the rates of hydrogen atom abstractions follow a linear free energy relationship[20] with the homolytic BDE of the bond being broken. Increasing interest in HAT reactions by transition-metal−oxo complexes has led to numerous studies that have supported similar correlations, even with substrates of different sizes. In one example, an excellent linear rate/BDE correlation was observed for a HAT from toluene, ethylbenzene, and cumene to a Ru=O complex, despite the steric difference in the substrates.[14a]

In contrast, the rates of intermolecular HAT reported here do not correlate with the bond enthalpy of the bond being broken, since **1**·^{t}**Bupy** reacts at very different rates with substrates of similar bond dissociation energies. *Instead, we propose that the main factor controlling the HAT rate is the steric accessibility of the C−H bond to the reactive nitrogen atom.* We used two series of substrates with very similar C−H bond energies and differing steric demands to illustrate this trend: HAT rate constants decrease in the order CHD > Me_2CHD > Me_4CHD ≈ 0 for the methyl-substituted cyclohexadiene series and CHD > dihydronaphthalene (DHN) > dihydroanthracene (DHA) ≈ 0 for the benzo-substituted cyclohexadiene series. In other words, as the number and size of substituents near the weak C−H bond increases, the rate decreases drastically. The rate of HAT drops by a factor of 50−90 from CHD to Me_2CHD or DHN, and further substitution to Me_4CHD or DHA renders the substrate completely unreactive.

There are other examples of systems in which the log k_{HAT}/BDE relationship does not hold for large substrates, although the effect is much less pronounced than the HAT reactivity of **1**·^{t}**Bupy**. The HAT rate by an octahedral *trans*-dioxoruthenium(VI) complex showed a linear (log k_{HAT})/(C−H BDE) relationship for a series of para-substituted phenols, with the exception of 2,6-di-*tert*-butyl-substituted substrates.[70] The rate of HAT from phenol was 4 times faster than from 2,6-di-*tert*-butylphenol, despite the opposite order of O−H BDE values (phenol > 2,6-di-*tert*-butylphenol by ∼5 kcal/mol). A similar trend is seen in the rates of reaction of phenols with peroxy and alkyl radicals, in which substituting the phenol substrate with two *o*-methyl groups slowed the HAT rate by a factor of ∼2, and substituting with two *o*-*tert*-butyl groups slowed the HAT rate by ∼100-fold.[71] A ruthenium(IV) sulfilamido species showed a good rate/BDE correlation in the HAT reaction with xanthene, CHD, DHA, and fluorene, but diphenylmethane and triphenylmethane reacted, respectively, about 20 and 50 times slower than the trend would predict based on BDE alone.[72] A putative Fe^{IV}=O intermediate reacted with fluorene and DHA in 80% yield, but not at all with diphenylmethane, indicating that substrate access to the Fe=O might be rate-limiting.[73] A recent review describes the range of selectivity factors (including sterics) controlling C−H activation reactions of organic molecules.[74]

The large difference in HAT rates of CHD versus Me_2CHD and CHD versus dihydronaphthalene with **1**·^{t}**Bupy** is among the most sensitive steric constraints observed for HAT reactions. We attribute this in part to the presence of a large imido N-substituent, which, in combination with the bulky β-diketiminate ligand, creates a substrate pocket to which access is greatly hindered. The added steric hindrance from the coordinated pyridine in the active species, **1**·^{t}**Bupy**, is also likely to play a role in limiting the size of the substrate binding site.

It is difficult to explain the 120-fold difference in the HAT rate constants between indene ($1.9(2) \times 10^{-2}$ M^{-1} s^{-1}) and dihydronaphthalene ($1.56(4) \times 10^{-4}$ M^{-1} s^{-1}) using a steric argument. This difference also cannot be explained by a difference in homolytic BDEs, because the C−H BDE of indene (calcd 77 kcal/mol) is larger than that of dihydronaphthalene (calcd 72 kcal/mol). A more likely explanation is the difference between the *heterolytic* bond enthalpies: deprotonating the hydrocarbon is calculated to be significantly easier for indene (calcd 351 kcal/mol) than dihydronaphthalene (calcd 366 kcal/mol). The correlation with heterolytic BDEs suggests that there is proton-transfer character in the transition state for HAT, with buildup of positive charge on the metal fragment and negative charge on the hydrocarbyl fragment. This is equivalent to stating that proton transfer and electron transfer are concerted but asynchronous, with proton

transfer slightly preceding electron transfer. A third way of expressing this idea is that the imido ligand has some Brønsted base character during the HAT reaction.[1f,75]

Gaining additional evidence for this idea was challenging because the sensitivity of the imidoiron complex prevented us from directly probing the proton affinity or the redox potentials of **1** or **1**·^{t}**Bupy**. Therefore, two alternative tests were used. First, in a HAT step with asynchronous proton and electron transfer, the charge buildup in the transition state should be stabilized by a more polar environment. This hypothesis was tested by performing the HAT reaction between **1**·^{t}**Bupy** and CHD in a solvent with added electrolyte. We found that the HAT rate constant k_{inter} is a factor of 1.60(9) larger in THF-d_8 containing 0.13 M [^{n}Bu$_4$N][BAr$^F{}_4$] ($1.16(4) \times 10^{-2}$ M^{-1} s^{-1}) than in neat THF-d_8 ($7.2(3) \times 10^{-3}$ M^{-1} s^{-1}) (Supporting Information Figure S-8). The faster rate in a solvent of higher ionic strength is consistent with charge buildup in the transition state. Second, we varied the basicity of the coordinated pyridine, as described above. Even after correcting for the differences in equilibrium binding constants, the more electron-donating pyridines gave a larger rate constant for intramolecular HAT (Figure 3). This trend is consistent with the idea that **1**·^{t}**Bupy** has basic character in the HAT reaction, because electron-donating groups on the ligands are expected to increase the basicity and hence the reactivity.

Steric Constraints on the HAT Transition State. Intermolecular HAT reactions involving metal−oxo complexes typically have positive $\Delta H^{\ddagger}$ values (on the order of 5−30 kcal/mol) and large negative $\Delta S^{\ddagger}$ values (on the order of −20 to −50 cal/mol·K).[13b,17,18b,19d,69a] For the HAT reactions reported here, the activation enthalpies of $\Delta H^{\ddagger}_{intra}$ = 14.6(5) kcal/mol and $\Delta H^{\ddagger}_{inter}$ = 14.4(8) kcal/mol are positive, and the values of $\Delta S^{\ddagger}_{intra}$ = −18(2) cal/mol·K and $\Delta S^{\ddagger}_{inter}$ = −9(3) cal/mol·K are negative. It is somewhat surprising that the activation parameters for the intramolecular and intermolecular reactions are similar in magnitude, and that the values of $\Delta S^{\ddagger}_{HAT}$ are not as negative as other HAT reactions, such as $\Delta S^{\ddagger}_{HAT}$ = −25 to −37 cal/mol·K for phenol HAT to a (corrole)Mn=NTs complex.[76] It is possible that the significant steric hindrance in the ground state of **1**·^{t}**Bupy** is somewhat relieved by lengthening the Fe−N$_{imido}$ bond to ∼1.90 Å in the HAT transition state, and this in turn gives greater flexibility. However, the value for the entropy of activation should be viewed with due caution because $\Delta S^{\ddagger}_{HAT}$ is derived from extrapolation to $1/T = 0$ of the quotient of two measured values (K_{eq} and k_{obs}) that each have experimental uncertainty.

The rate of the HAT reaction had a surprisingly large dependence on the size of the substrate. As described in the Results section, the rate for CHD was about 50 times larger than that for 1,4-dihydronaphthalene (DHN), and 9,10-dihydroanthracene (DHA) did not undergo HAT. To evaluate these reactions computationally, HAT transition states for C−H activation of DHN and DHA were calculated using the same ONIOM(B3LYP/6-311++G(d,p)) level of theory employed for the CHD reaction coordinate. The calculated quartet transition states for CHD, DHN, and DHA all place the substrate roughly in the equatorial plane defined by the β-diketiminate and imido nitrogens and slightly away from the ^{t}Bupy donor ligand (Supporting Information Figure S-13). The second ring of a DHN substrate can position itself on the distal side of the equatorial plane (away from ^{t}Bupy) with minimal additional steric congestion. However, the addition of a third ring to the substrate, as in DHA, leads to steric hindrance with the ^{t}Bupy and 2,6-diisopropylphenyl substituents. The larger substrates have higher calculated free energy barriers: $\Delta\Delta G^{\ddagger}(\text{DHN} - \text{CHD})_{calcd}$ = 1.1 kcal/mol, $\Delta\Delta G^{\ddagger}(\text{DHA} - \text{CHD})_{calcd}$ = 7.0 kcal/mol, consistent with the experimentally observed selectivity patterns. Analysis of the MM portion of the ONIOM extrapolated energy yields $\Delta\Delta E^{\ddagger}(\text{DHN} - \text{CHD})_{calcd}$ = 0.9 kcal/mol, $\Delta\Delta E^{\ddagger}(\text{DHA} - \text{CHD})_{calcd}$ = 4.3 kcal/mol. Assuming that there is a rough cancellation of entropic and enthalpic corrections to the free energy, these simulations support the experimental hypothesis that steric factors are primarily responsible for the selectivity observed in HAT reactions of **1**·^{t}**Bupy**.

Dependence of HAT on the Iron Coordination Number. We now consider an intriguing question: why is four-coordinate **1**·^{t}**Bupy** so much reactive than three-coordinate **1**? Coordination-induced rate enhancement is not a unique phenomenon: the rate of HAT and other reactions of oxo and nitrido complexes can be accelerated by pyridine,[77] pyridine *N*-oxide,[78] and halide[79] additives. Although **1** does react with CHD to form **2** and benzene, the reaction is much slower (requiring hours at room temperature) than the reaction of **1**·^{t}**Bupy** and CHD to form **2**·^{t}**Bupy** (requiring minutes at −51 °C). There are several potential explanations for why pyridine coordination could magnify the HAT rate.

Hypothesis 1: Coordination of ^{t}Bupy Weakens the Fe=N π-Bond. One possibility is based on the >0.06 Å increase in M−L bond length upon coordinating ^{t}Bupy, demonstrated quantitatively in the computations on **1** and **1**·^{t}**Bupy**. Lengthening the Fe−imido bond decreases orbital overlap and weakens π-donation of the imido ligand into metal d orbitals. Thus, a longer Fe−N bond predicts a buildup of electron density on the imido ligand in **1**·^{t}**Bupy**, which would magnify the rate of HAT reactions like this one that have basic character at the imido nitrogen (see above).

This explanation is consistent with literature observations on iron−oxo complexes. The axial thiolate in heme enzymes increases the basicity of the oxo ligand and makes it more effective for HAT.[80] In non-heme oxoiron(IV) complexes as well, faster HAT rates correlate with a more basic trans ligand,[12a,83b] and with longer Fe=O bonds.[12e] A similar dependence of HAT rate on axial ligand basicity is evident in corrolazine-ligated oxomanganese(V) complexes.[79]

Hypothesis 2: Coordination of ^{t}Bupy Bends the Fe=N−C Linkage. In a second view, the bent Fe=N−C angle in the ground state of **1**·^{t}**Bupy** is more closely matched to the HAT transition state geometry than is the corresponding Fe=N−C angle in ground-state **1**. This would lead to a faster rate for **1**·^{t}**Bupy** than **1** due to the smaller structural reorganization energy.[81] This explanation would fit into models of HAT reactions conforming to the Marcus picture of electron transfer.[75] Computations do indicate that the Fe=N−C angle in **1**·^{t}**Bupy** (169° for quartet, 162° for sextet) is somewhat closer to the four-coordinate transition state (143° for the quartet, 140° for the sextet) than the Fe=N−C angle in **1** (173° for quartet, 163° for sextet) is to the corresponding three-coordinate transition state (138° for quartet, 139° for the sextet). However, these geometric differences are small and unlikely to be the major contributor to the huge difference in reactivity between **1** and **1**·^{t}**Bupy**. Furthermore, computational studies have shown that bending the M=N−R linkage is not energetically costly.[82]

Hypothesis 3: Coordination of ^{t}Bupy Allows Reaction on a Different Spin-State Surface. Spin-state-dependent reactivity is a model that has been very useful in understanding HAT to iron(IV)−oxo complexes.[12,83,84] Many non-heme oxoiron(IV) complexes have an intermediate ($S = 1$) ground spin state, with a

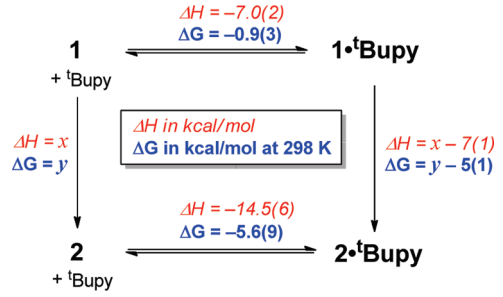

Figure 9. Thermodynamic square relating pyridine binding to HAT enthalpies and free energies.

low-lying high-spin (S = 2) excited state.[85] In these systems, computations suggest that spin crossover is important at the HAT transition state, since the reaction on the quintet surface has a lower barrier than the triplet surface.[83] Thus, an accessible high-spin state is thought to facilitate HAT in these complexes. Magnetic susceptibility, EPR, and computational data show that the ground state in compound **1** is intermediate spin (S = 3/2), and the computational model places the high-spin state higher in energy (+12 kcal/mol). Addition of pyridine to **1** does bring the S = 3/2 and S = 5/2 spin states to similar energy (computed to be within 2 kcal/mol); however, in contrast to the octahedral oxoiron(IV) systems, the calculated energy of the lowest transition state for HAT by **1**·^{t}**Bupy** *does not differ significantly by spin state*. Therefore, our computational results do not support the idea of spin-state-dependent reactivity in this iron system.

Hypothesis 4: HAT by 1·^{t}Bupy is More Exothermic because ^{t}Bupy Binds to 2 More Strongly Than to 1. The Hammond postulate[86] suggests that the faster HAT rate for **1**·^{t}**Bupy** might follow from a greater driving force for HAT in the pyridine adducts. This driving force may be quantified by comparing the thermodynamics of ^{t}Bupy coordination to **1** and to **2** and subsequently constructing a thermodynamic square (Figure 9). Using the same method described above for quantifying the equilibrium of **1** and **1**·^{t}**Bupy**, we determined K_{eq} for ^{t}Bupy coordination to **2** over the temperature range of 25−110 °C in toluene-d_8. The van't Hoff plot (Supporting Information Figure S-11) gives ΔH_{eq}° = −14.5(6) kcal/mol and ΔS_{eq}° = −30(1) cal/mol·K for the equilibrium of **2** and **2**·^{t}**Bupy**, which corresponds to ΔG_{eq}° = −5.6(9) kcal/mol at 298 K. Because of the constraint imposed by the thermodynamic square, HAT by **1**·^{t}**Bupy** must therefore be 5(1) kcal/mol more exergonic and 7(1) kcal/mol more exothermic than HAT by **1** at 298 K. Thus, pyridine binding indeed makes HAT more thermodynamically favorable.

We also sought to quantify the effect of ^{t}Bupy on $\Delta H^{\ddagger}$ and $\Delta G^{\ddagger}$ of the HAT reaction, to test whether or not the kinetic effect of ^{t}Bupy on the HAT rate follows the thermodynamic effect of stronger binding to **2** than **1**. Thus, we performed HAT reactions between **1** and CHD *without* ^{t}Bupy. An Eyring plot of the second-order rate constant k_{inter} for this reaction between 25 and 55 °C (Supporting Information Figure S-12) gives the activation parameters for the HAT reaction without ^{t}Bupy of $\Delta H^{\ddagger}$ = +12.2(3) kcal/mol, $\Delta S^{\ddagger}$ = −33(2) cal/mol·K, and $\Delta G^{\ddagger}$ = +22(1) kcal/mol at 298 K. Thus, the addition of ^{t}Bupy results in a drop in HAT barrier height by $\Delta\Delta G^{\ddagger}$ = −5(2) kcal/mol, which is the similar to the thermodynamic driving force. In summary, the magnitude of change in thermodynamics for the HAT reactions with and without pyridine is sufficient to explain the change in rate, if the thermodynamic stabilization of binding in the product is already realized in the transition state.

Thus, a combination of experimental data, computational results, and chemical principles *support both hypotheses 1 and 4*. In hypothesis 1, coordination of a fourth ligand gives weakening of the Fe═NR bond. In this explanation, the basicity of the pyridine is "relayed" through the iron to the imido group, which abstracts a hydrogen atom through a transition state with proton transfer character. It is reasonable that the current system has at least as much dependence on basicity as the well-studied oxoiron(IV) species,[84] because of the lower formal oxidation state of these imido complexes (Fe^{3+} vs Fe^{4+}) and the lesser electronegativity of nitrogen as compared to oxygen.[87] In hypothesis 4, HAT becomes faster with an added pyridine donor because coordination of pyridine to the product amido complex **2** is stronger than coordination to imido **1**, providing a thermodynamic driving force for HAT. A explanation similar to hypothesis 4 for rate enhancement by added ligands was presented recently in the context of oxomanganese chemistry.[79]

Limitations and Implications. How potent is the iron(III) imido complex for HAT? A clue comes from the observation that the intramolecular HAT reaction breaks a C−H bond of the diisopropylphenyl substituent in the β-diketiminate ligand. Assuming the BDE of the isopropyl methine C−H is similar to that in cumene (~86 kcal/mol),[88] **1**·^{t}**Bupy** is thermodynamically capable of breaking C−H bonds significantly stronger than those in CHD (71 kcal/mol). However, the "effective concentration" of isopropyl groups in **1**·^{t}**Bupy** is huge, since there are always four methine protons near the metal. Thus, even added substrates with a similar BDE would need to be in a large excess in solution to compete kinetically with intramolecular ligand activation. It is also possible that fast trapping of the benzylic radical by the diketiminate backbone drives the intramolecular HAT reaction. Current efforts are devoted to the design of ligands that will not be attacked by the reactive imido fragment, in order to harness the full thermodynamic potential of imidoiron(III) species for C−H activation reactions.

Although ligand activation limits the substrate scope of intermolecular HAT by **1**·^{t}**Bupy**, this work is important because it shows that sterically bulky, weak-field supporting ligands can produce low-coordinate complexes that are reactive toward homolytic C−H bond cleavage. It is noteworthy that other late transition metal oxo and imido complexes that are reactive toward HAT are also supported by weak-field ligand frameworks,[12,25d,31] suggesting that the use of weak-field (π-donor) ligands may be a general advantage in the design of ligand systems for productive HAT processes.

■ CONCLUSIONS

The ability of bulky ligands to stabilize a reactive Fe═NR species has enabled the first in-depth study of the mechanism of H-atom transfer (HAT) reactivity of an imidoiron complex. The imido complex L^{Me}Fe═NAd (**1**) reversibly coordinates ^{t}Bupy, forming the highly reactive four-coordinate imido complex L^{Me}Fe═NAd(^{t}Bupy) (**1**·^{t}**Bupy**). Complex **1**·^{t}**Bupy** activates small substrates with weak C−H bonds (e.g., CHD and indene), as well as the methine C−H on its own supporting ligand. In each case, the iron−amido complex resulting from HAT was observed. Significantly, **1**·^{t}**Bupy** abstracts hydrogen atoms even at −51 °C.

Mechanistic studies were used to elucidate the details of the HAT reaction. Large H/D KIEs of ≥80 in the intermolecular

dx.doi.org/10.1021/ja2005303 |*J. Am. Chem. Soc.* 2011, 133, 9796–9811

reactions with CHD and indene demonstrate rate-limiting C−H cleavage. The magnified reactivity of the four-coordinate iron-imido complex **1**·^{t}**Bupy** is partly attributed to a "push" effect where coordination of pyridine gives a longer Fe═N bond and more basic imido nitrogen atom in the starting material, and pyridine also stabilizes the amidoiron(II) product of the reaction. The basicity of the imido nitrogen atom is important for HAT,[22i] because there is charge buildup in the HAT transition state that gives the HAT some proton-transfer character. Spin-state-dependent reactivity does not appear to be an important factor in these HAT reactions.

The potency of **1**·^{t}**Bupy** toward HAT attests to the potential of low-coordinate imido complexes with weak-field ligands for C−H activation reactions. The considerable steric demands of the supporting diketiminate ligand and large imide N-substituent cause the imido complex to strongly prefer unhindered substrates in HAT reactions. This sterically controlled reactivity is significant because it represents a deviation from the typical linear free energy relationships, where selectivity is determined primarily by the C−H bond dissociation energy. In a system that can activate stronger C−H bonds, one may be able to use this steric control to develop catalysts that use nitrene-based intermediates to selectively target the stronger, but more sterically accessible, primary C−H bonds of organic compounds.

EXPERIMENTAL SECTION

General Considerations. All air-sensitive manipulations were performed under a nitrogen atmosphere in an MBraun glovebox maintained below 1 ppm of O_2 and H_2O, or on a double-manifold vacuum line using standard Schlenk techniques. For air-sensitive manipulations, all glassware was dried overnight at 150 °C. 1-Azidoadamantane was purchased from Aldrich and crystallized twice from pentane prior to use. 1,4-Cyclohexadiene and indene were purchased from Aldrich and vacuum-transferred from CaH_2 and stored over 3 Å molecular sieves (activated at ∼350 °C for 12 h under vacuum). 4-*tert*-Butylpyridine and 4-trifluoromethylpyridine were purchased from Aldrich and degassed and dried over activated 3 Å molecular sieves prior to use. 4-Dimethylaminopyridine and 4-phenylpyridine were purchased from Aldrich and recrystallized from toluene prior to use. 1,4-Dihydronaphthalene was purchased from TCI and vacuum-transferred from CaH_2. 1,4-Dimethyl-1,4-cyclohexadiene[89] and 1,2,4,5-tetramethyl-1,4-cyclohexadiene[90] were prepared by literature methods. L^{Me}FeNAd (**1**) was prepared as previously described.[38] Other reagents were obtained commercially and used without purification. Benzene-d_6 was dried over flame-activated alumina, and toluene-d_8 was vacuum-transferred from a purple sodium benzophenone ketyl and stored over Na metal. Before use, an aliquot of each solvent was qualitatively tested for dryness with a drop of THF containing sodium benzophenone ketyl. NMR data were collected on either a Bruker Avance 400 or Bruker Avance 500 spectrometer. ^{1}H NMR spectra are referenced to residual C_6D_5H (δ 7.16 ppm), C_7D_7H (δ 2.08 ppm), or TMS (δ 0.00 ppm). ^{2}H NMR spectra are referenced to a small added quantity of $CDCl_3$ (δ 7.26 ppm). The NMR probe temperature for the variable-temperature measurements was calibrated using neat ethylene glycol or methanol.[91] Mass spectral data were obtained on a Shimadzu QP2010 system with electron impact ionization.

Octadeutero-1,4-cyclohexadiene (CHD-d_8). In our hands, the published procedure[92] using NH_3 solvent gave the incompletely deuterated product $C_6D_6H_2$. A modified procedure using ND_3 is given here, which gives the fully deuterated product C_6D_8. A small three-neck flask equipped with a dry ice/acetone condenser was thoroughly flushed with nitrogen, and ND_3 was condensed into the flask (∼15 mL). Ethanol-d_1 (2.7 mL, 46 mmol), benzene-d_6 (1.5 mL, 16.9 mmol), and triglyme (5 mL) were added to the liquid ND_3 via syringe, and the mixture was equilibrated to −40 °C in a MeCN/dry ice bath. Dry sodium metal (1.17 g, 51 mmol) was cut into small pieces and added in portions over a 2 h period to the vigorously stirring reaction mixture by opening a stopper on the flask against a positive pressure of N_2. After an additional 30 min, the reaction was warmed to room temperature to evaporate the ammonia, and the reaction was slowly and carefully quenched with D_2O until the excess sodium metal was consumed and effervescence ceased. The reaction mixture was transferred to a separatory funnel and washed with water (3 × 50 mL). After draining the aqueous layer the final time, the neat product was removed from the separatory funnel by pipet and transferred to a bomb flask containing CaH_2. The mixture was freeze−pump−thaw degassed three times and stirred for 24 h, after which the product was vacuum-transferred to a storage container containing activated 3 Å molecular sieves. The yield was 1.18 g (79%). ^{1}H NMR (400 MHz, $CDCl_3$): no peaks. ^{2}H NMR (61 MHz, $CHCl_3$): δ 2.68 (s, 4D), 4.81 (s, 4D) ppm. EI-MS$^+$ (assignment, rel intensity): m/z 82 ([M − 3D]$^+$, 45%), 86 ([M − D]$^+$, 100%), 88 (M$^+$, 93%).

1,1,3-Trideuteroindene (Indene-d_3). The synthesis of indene-d_3 was adapted from a known method.[93] Freshly distilled indene (13.1 g, 113 mmol) was heated to 100 °C in a bomb flask with DBU (1.7 mL, 11.3 mmol), D_2O (20.5 mL, 1.13 mol), and *p*-dioxane (20 mL). After 24 h, the reaction mixture was cooled and transferred to a separatory funnel. The organic layer was washed with brine (200 mL), a 50:50 solution of 1 M HCl/brine (200 mL), and brine (2 × 200 mL). The neat oil was then removed and distilled under reduced pressure. The recovered indene was recycled, and the DBU/D_2O/dioxane reaction was repeated for a total of three iterations. The final recovered material (9.16 g, 68%) was 98.7% d_3-labeled by ^{1}H NMR integration. Before use, the indene-d_3 was distilled from CaH_2 and stored over activated 3 Å molecular sieves. ^{1}H NMR (400 MHz, $CDCl_3$): δ 7.47 (d, 1H), 7.40 (d, 1H), 7.25 (m, 1H), 7.18 (m, 1H), 6.55 (s, 1H). ^{2}H NMR (61 MHz, $CHCl_3$): δ 6.88 (s, 1D), 3.38 (s, 2D) ppm. EI-MS$^+$ (assignment, rel intensity): m/z 117 ([M − D]$^+$, 34%), 118 ([M − H]$^+$, 72%), 119 (M$^+$, 100%).

Equilibrium Studies. An NMR tube was loaded with 0.5 mL of an 18 mM solution of **1** in C_7D_8, and the tube was sealed with a rubber septum. The NMR probe was equilibrated at the given temperature, the given quantity of pyridine was added via microsyringe, and the tube was vigorously shaken. (Note: for low-temperature measurements, the NMR sample was precooled in an acetone/dry ice bath prior to inserting into the probe in order to decrease the time to reach temperature equilibrium in the NMR probe.) The sample was allowed to equilibrate in the probe for ca. 2−3 min, and the ^{1}H NMR spectrum was recorded. This procedure was repeated for several different concentrations of [^{t}Bupy]$_0$, and the change in chemical shift of a selected resonance was plotted as a function of [^{t}Bupy]$_0$. The formula in eq 9 was used to fit the data in order to extract the value of K_{eq}.

$$\Delta\delta \approx \left(\frac{K_{eq}[^t\mathrm{Bupy}]_0}{1 + K_{eq}[^t\mathrm{Bupy}]_0}\right) \qquad (9)$$

Intermolecular HAT Kinetic Experiments. An NMR tube was loaded with **1** in toluene-d_8, the given amount of substrate, and a capillary filled with a known amount of cobaltocene in toluene-d_8 and sealed with a rubber septum. The tube was cooled to −78 °C in a dry ice/acetone bath, and the given amount of ^{t}Bupy was added via microsyringe. The tube was quickly shaken to ensure mixing, the sample was quickly inserted into the NMR spectrometer (the probe was pre-equilibrated to −51 °C), and the kinetic acquisition program was started. Generally the first 2−3 data points were discarded to ensure the sample had completely equilibrated to −51 °C. A plot of the concentration of **1**·^{t}**Bupy** (y) versus reaction time (t) was analyzed with Kaleidagraph v. 3.51.[43] These data were fit to the general first-order

dx.doi.org/10.1021/ja2005303 |J. Am. Chem. Soc. 2011, 133, 9796–9811

integrated kinetic equation $[\mathbf{1}] = a + [b \exp(-k_{obs}t)]$, where a and b are constants and k_{obs} is the pseudo-first-order rate constant.

Computational Details. The Gaussian 09 package[94] was used for this research unless noted otherwise. The B3LYP hybrid functional was employed.[95] Hybrid quantum mechanics/molecular mechanics (QM/MM) calculations were used to study full experimental models of the imido intermediates **1** and **1**·^{t}**Bupy**. The QM/MM calculations utilized the ONIOM[96] methodology within the Gaussian suite of programs. The B3LYP/6-311++G(d,p) level of theory was applied to the QM region; the MM region included the bulky substituents (Ar and Me substituents of L^{Me} and the entire adamantyl group except the carbon directly attached to the imido nitrogen). The MM interactions were modeled with the universal force field (UFF).[97]

Simulations did not use any symmetry restraints, and several different initial guess and SCF convergence schemes were employed to help ensure the isolation of the lowest energy state of a particular multiplicity. Reactant, transition state, and product geometries were fully optimized using gradient methods. The unrestricted Kohn−Sham formalism was used for the description of all open-shell species, unless otherwise noted. The energy Hessian was calculated and thus confirmed the calculated stationary points as minima (no imaginary frequencies) or transition states (one imaginary frequency). All reported enthalpies are calculated at 1 atm and 298.15 K.

GC/MS Detection of Organic Products. Representative reactions with CHD, Me_2CHD, DHN, and indene were analyzed by GC/MS to determine the yields of organic HAT byproducts by the following method. At the end of the reaction (>95% consumption of complex **1** by ^{1}H NMR spectroscopy), the NMR sample was exposed to air and poured onto a packed silica gel column (0.5 cm ×6 cm). Organic products were eluted with ∼10 mL toluene, and the mixture was spiked with 0.10 mL mesitylene. GC integration of the HAT byproduct was compared to mesitylene to derive the yield of the organic product.

■ ASSOCIATED CONTENT

Supporting Information. Kinetic data, Arrhenius plots, computational details, and complete ref 94. This material is available free of charge via the Internet at http://pubs.acs.org.

■ AUTHOR INFORMATION

Corresponding Author
holland@chem.rochester.edu; t@unt.edu

■ ACKNOWLEDGMENT

The authors thank Prof. James Mayer for helpful discussions. P.L.H. acknowledges financial support from the Petroleum Research Fund (44942-AC) and the National Science Foundation (CHE-0911314). R.E.C. acknowledges the NSF (Graduate Research Fellowship) and the University of Rochester (Elon Hooker Fellowship). T.R.C. acknowledges financial support from the Department of Energy (DE-FG02-03ER15387). Calculations employed the UNT computational chemistry resource, for which we acknowledge the NSF for support through CRIF Grant CHE-0741936.

■ REFERENCES

(1) (a) Hodgkiss, J. M.; Rosenthal, J.; Nocera, D. G. In *Hydrogen-Transfer Reactions*; Hynes, J. T., Klinman, J. P., Limbach, H.-H., Schowen, R. L., Eds.; Wiley-VCH: Weinheim, Germany, 2007; Vol. 2, pp 503−562. (b) Schöneich, C. In *Hydrogen-Transfer Reactions*; Hynes, J. T., Klinman, J. P., Limbach, H.-H., Schowen, R. L., Eds.; Wiley-VCH: Weinheim, Germany, 2007; Vol. 3, pp 1013−1036. (c) Mayer, J. M. *Annu. Rev. Phys. Chem.* **2004**, *55*, 363–390. (d) Hammes-Schiffer, S. *ChemPhysChem* **2002**, *3*, 33–42. (e) Huynh, M. H. V.; Meyer, T. J. *Chem. Rev.* **2007**, *107*, 5004–5064. (f) Warren, J. J.; Tronic, T. A.; Mayer, J. M. *Chem. Rev.* **2010**, *110*, 6961–7001.

(2) In the strictest definition, HAT is a subset of proton-coupled electron-transfer (PCET) reactions when the proton and electron derive from the same bond (see ref 1e). In this paper we use the term "HAT" to describe the transformation in eq 1, in order to specify *single-step* HAT rather than *stepwise* proton/electron transfer. See ref 1f for further discussion on this topic.

(3) (a) Gunay, A.; Theopold, K. H. *Chem. Rev.* **2010**, *110*, 1060–1081. (b) Borovik, A. S. *Chem. Soc. Rev.* **2011**, *40*, 1870–1874.

(4) (a) Ortiz de Montellano, P. R., Ed. *Cytochrome P-450: Structure, Mechanism and Biochemistry*, 3rd ed.; Plenum Publishers: New York, 2005. (b) Sono, M.; Roach, M. P.; Coulter, E. D.; Dawson, J. H. *Chem. Rev.* **1996**, *96*, 2841–2888. (c) Meunier, B.; de Visser, S. P.; Shaik, S. *Chem. Rev.* **2004**, *104*, 3947–3980.

(5) (a) Ragsdale, S. W. *Chem. Rev.* **2006**, *106*, 3317–3337. (b) Baik, M.-H.; Newcomb, M.; Friesner, R. A.; Lippard, S. J. *Chem. Rev.* **2003**, *103*, 2385–2419.

(6) (a) Stubbe, J.; Nocera, D. G.; Yee, C. S.; Chang, M. C. Y. *Chem. Rev.* **2003**, *103*, 2167–2201. (b) Hynes, J. T.; Klinman, J. P.; Limbach, H.-H.; Schowen, R. L., Eds. *Hydrogen-Transfer Reactions*; Wiley-VCH: Weinheim, Germany, 2007; Vol. 4, pp 1473−1495.

(7) Liang, Z.-X.; Klinman, J. P. *Curr. Opin. Struct. Biol.* **2004**, *14*, 648–655.

(8) (a) Baldwin, J. E.; Bradley, M. *Chem. Rev.* **1990**, *90*, 1079–1088. (b) Schenk, W. A. *Angew. Chem., Int. Ed.* **2000**, *39*, 3409–3411.

(9) (a) Krebs, C.; Fujimori, D. G.; Walsh, C. T.; Bollinger, J. M. *Acc. Chem. Res.* **2007**, *40*, 484–492. (b) Solomon, E. I.; Brunold, T. C.; Davis, M. I.; Kemsley, J. N.; Lee, S.-K.; Lehnert, N.; Neese, F.; Skulan, A. J.; Yang, Y.-S.; Zhou, J. *Chem. Rev.* **2000**, *100*, 235–349.

(10) Fujii, H. *Coord. Chem. Rev.* **2002**, *226*, 51–60.

(11) (a) Groves, J. T.; Haushalter, R. C.; Nakamura, M.; Nemo, T. E.; Evans, B. J. *J. Am. Chem. Soc.* **1981**, *103*, 2884–2886. (b) Groves, J. T.; Nemo, T. E. *J. Am. Chem. Soc.* **1983**, *105*, 5786–5791. (c) Groves, J. T.; Nemo, T. E. *J. Am. Chem. Soc.* **1983**, *105*, 6243–6248. (d) Chin, D.-H.; Balch, A.; La Mar, G. N. *J. Am. Chem. Soc.* **1980**, *102*, 1446–1448. (e) Chin, D.-H.; La Mar, G. N.; Balch, A. *J. Am. Chem. Soc.* **1980**, *102*, 5945–5947. (f) La Mar, G. N.; de Ropp, J. S.; Latos-Grazynski, L.; Balch, A. L.; Johnson, R. B.; Smith, K. M.; Parish, D. W.; Cheng, R.-J. *J. Am. Chem. Soc.* **1983**, *105*, 782–787. (g) Balch, A. L.; Chan, Y.-W.; Cheng, R.-J.; La Mar, G. N.; Latos-Grazynski, L.; Renner, M. R. *J. Am. Chem. Soc.* **1984**, *106*, 7779–7785.

(12) (a) Sastri, C. V.; Lee, J.; Oh, K.; Lee, Y. J.; Lee, J.; Jackson, T. A.; Ray, K.; Hirao, H.; Shin, W.; Halfen, J. A.; Kim, J.; Que, L.; Shaik, S.; Nam, W. *Proc. Natl. Acad. Sci. U.S.A.* **2007**, *49*, 19181–19186. (b) Paine, T. K.; Costas, M.; Kaizer, J.; Que, L. *J. Biol. Inorg. Chem.* **2006**, *11*, 272–276. (c) Que, L.; Tolman, W. B. *Nature* **2008**, *455*, 333–340. (d) Ray, K.; England, J.; Fiedler, A. T.; Martinho, M.; Münck, E.; Que, L. *Angew. Chem., Int. Ed.* **2008**, *47*, 8068–8071. (e) Decker, A.; Rohde, J.-U.; Klinker, E. J.; Wong, S. D.; Que, L.; Solomon, E. I. *J. Am. Chem. Soc.* **2007**, *129*, 15983–15996. (f) Fiedler, A. T.; Que, L. *Inorg. Chem.* **2009**, *48*, 11038–11047. (g) Klinker, E. J.; Shaik, S.; Hirao, H.; Que, L. *Angew. Chem., Int. Ed.* **2009**, *48*, 1291–1295. (h) England, J.; Martinho, M.; Farquar, E. R.; Frisch, J. R.; Bominaar, E. L.; Münck, E.; Que, L. *Angew. Chem., Int. Ed.* **2009**, *48*, 3622–3626. (i) Kaizer, J.; Klinker, E. J.; Oh, N. Y.; Rodhe, J.-U.; Song, W. J.; Stubna, A.; Kim, J.; Münck, E.; Nam, W.; Que, L. *J. Am. Chem. Soc.* **2004**, *126*, 472–473. (j) Jeong, Y. J.; Kang, Y.; Han, A.-R.; Lee, Y.-M.; Kotani, H.; Fukuzumi, S.; Nam, W. *Angew. Chem., Int. Ed.* **2008**, *47*, 7321–7324. (k) Kang, Y.; Chen, H.; Jeong, Y. J.; Lai, W.; Bae, E. H.; Shaik, S.; Nam, W. *Chem.—Eur. J.* **2009**, *15*, 10039–10046.

(13) (a) Jin, N.; Groves, J. T. *J. Am. Chem. Soc.* **1999**, *121*, 2923–2924. (b) Lansky, D. E.; Goldberg, D. P. *Inorg. Chem.* **2006**, *45*, 5119–5125.

(14) (a) Bryant, J. R.; Mayer, J. M. *J. Am. Chem. Soc.* **2003**, *125*, 10351–10361. (b) Bryant, J. R.; Matsuo, T.; Mayer, J. M. *Inorg. Chem.*

2004, *43*, 1587–1592. (c) Matsuo, T.; Mayer, J. M. *Inorg. Chem.* **2005**, *44*, 2150–2158.

(15) (a) Cook, G. K.; Mayer, J. M. *J. Am. Chem. Soc.* **1994**, *116*, 1855–1868. (b) Cook, G. K.; Mayer, J. M. *J. Am. Chem. Soc.* **1995**, *117*, 7139–7156.

(16) Waidmann, C. R.; Zhou, X.; Tsai, E. A.; Kaminsky, W.; Hrovat, D. A.; Borden, W. T.; Mayer, J. M. *J. Am. Chem. Soc.* **2009**, *131*, 4729–4743.

(17) (a) Gardner, K. A.; Mayer, J. M. *Science* **1995**, *269*, 1849–1851. (b) Gardner, K. A.; Kuehnert, L. L.; Mayer, J. M. *Inorg. Chem.* **1997**, *36*, 2069–2078.

(18) (a) Parsell, T. H.; Behan, R. K.; Green, M. T.; Hendrich, M. P.; Borovik, A. S. *J. Am. Chem. Soc.* **2006**, *128*, 8728–8729. (b) Parsell, T. H.; Yang, M.-Y.; Borovik, A. S. *J. Am. Chem. Soc.* **2009**, *131*, 2762–2763. (c) Gupta, R.; Borovik, A. S. *J. Am. Chem. Soc.* **2003**, *125*, 13234–13242.

(19) (a) Seok, W. K.; Meyer, T. J. *Inorg. Chem.* **2005**, *44*, 3931–3941. (b) Binstead, R. A.; McGuire, M. E.; Dovletoglou, A.; Seok, W. K.; Roecker, L. E.; Meyer, T. J. *J. Am. Chem. Soc.* **1992**, *114*, 173–186. (c) Gilbert, J. A.; Gersten, S. W.; Meyer, T. J. *J. Am. Chem. Soc.* **1982**, *104*, 6872–6873. (d) Gilbert, J.; Roecker, L.; Meyer, T. J. *Inorg. Chem.* **1987**, *26*, 1126–1132. (e) Binstead, R. A.; Meyer, T. J. *J. Am. Chem. Soc.* **1987**, *109*, 3287–3297. (f) Binstead, R. A.; Moyer, B. A.; Samuels, G. J.; Meyer, T. J. *J. Am. Chem. Soc.* **1981**, *103*, 2897–2889.

(20) (a) Bell, R. P. *Proc. R. Soc. London, Ser. A* **1936**, *154*, 414–429. (b) Evans, M. G.; Polanyi, M. *Trans. Faraday Soc.* **1935**, *31*, 875–894.

(21) Berry, J. F. *Comments Inorg. Chem.* **2009**, *30*, 28–66.

(22) Iron−imido complexes: (a) Brown, S. D.; Peters, J. C. *J. Am. Chem. Soc.* **2005**, *127*, 1913–1923. (b) Brown, S. D.; Betley, T. A.; Peters, J. C. *J. Am. Chem. Soc.* **2003**, *125*, 322–323. (c) Betley, T. A.; Peters, J. C. *J. Am. Chem. Soc.* **2003**, *125*, 10782–10783. (d) Bart, S. C.; Lobkovsky, E.; Bill, E.; Chirik, P. J. *J. Am. Chem. Soc.* **2006**, *128*, 5302–5303. (e) Mehn, M. P.; Brown, S. D.; Jenkins, D. M.; Peters, J. C.; Que, L. *Inorg. Chem.* **2006**, *45*, 7417–7427. (f) Lu, C. C.; Saouma, C. T.; Day, M. W.; Peters, J. C. *J. Am. Chem. Soc.* **2007**, *129*, 4–5. (g) Verma, A. K.; Nazif, T. N.; Achim, C.; Lee, S. C. *J. Am. Chem. Soc.* **2000**, *122*, 11013–11014. (h) Thomas, C. M.; Mankad, N. P.; Peters, J. C. *J. Am. Chem. Soc.* **2006**, *128*, 4956–4957. (i) Nieto, I.; Ding, F.; Bontchev, R. P.; Wang, H.; Smith, J. M. *J. Am. Chem. Soc.* **2008**, *130*, 2716–2717. (j) Ni, C.; Fettinger, J. C.; Long, G. J.; Brynda, M.; Power, P. P. *Chem. Commun.* **2008**, 6045–6047. (k) Scepaniak, J. J.; Young, J. A.; Bontchev, R. P.; Smith, J. M. *Angew. Chem., Int. Ed.* **2009**, *48*, 3158–3160. (l) Moret, M.-E.; Peters, J. C. *Angew. Chem., Int. Ed.* **2011**, *50*, 2063–2067. (m) King, E. R.; Hennessey, E. T.; Betley, T. A. *J. Am. Chem. Soc.* **2011**, *133*, 4917–4923.

(23) Ruthenium−imido complexes: (a) Walstrom, A. N.; Fullmer, B. C.; Fan, H.; Pink, M.; Buschhorn, D. T.; Caulton, K. G. *Inorg. Chem.* **2008**, *47*, 9002–9009. (b) Leung, S. K.-Y.; Tsui, W.-M.; Huang, J.-S.; Che, C.-M.; Liang, J.-L.; Zhu, N. *J. Am. Chem. Soc.* **2005**, *127*, 16629–16640. (c) Danopoulos, A. A.; Wilkinson, G.; Hussain-Bates, B.; Hursthouse, M. B. *Polyhedron* **1992**, *11*, 2961–2964. (d) Burrell, A. K.; Steedman, A. J. *Chem. Commun.* **1995**, 2109–2110. (e) Burrell, A. K.; Steedman, A. J. *Organometallics* **1997**, *16*, 1203–1208. (f) Fantauzzi, S.; Gallo, E.; Caselli, A.; Ragaini, F.; Casati, N.; Macchi, P.; Cenini, S. *Chem. Commun.* **2009**, 3952–3954. (g) Takaoka, A.; Gerber, L. C. H.; Peters, J. C. *Angew. Chem., Int. Ed.* **2010**, *49*, 4088–4091.

(24) Osmium−imido complexes: (a) Michelman, R. I.; Andersen, R. A.; Bergman, R. G. *J. Am. Chem. Soc.* **1991**, *113*, 5100–5102. (b) Michelman, R. I.; Bergman, R. G.; Andersen, R. A. *Organometallics* **1993**, *12*, 2741–2751. (c) Lutz, C. M.; Wilson, S. R.; Shapley, P. A. *Organometallics* **2005**, *24*, 3350–3353. (d) Danopoulos, A. A.; Wilkinson, G.; Hussain-Bates, B.; Hursthouse, M. B. *J. Chem. Soc., Dalton Trans.* **1991**, 1855–1860. (e) Nugent, W. A.; Harlow, R. L.; McKinney, R. J. *J. Am. Chem. Soc.* **1979**, *101*, 7265–7268. (f) Muñiz, K.; Nieger, M.; Mansikkamäki, H. *Angew. Chem., Int. Ed.* **2003**, *42*, 5958–5961. (g) Griffith, W. P.; McManus, N. T.; Skapski, A. C.; White, A. D. *Inorg. Chim. Acta* **1985**, *105*, L11. (h) Shapley, P. A.; Own, Z.-Y.; Huffman, J. C. *Organometallics* **1986**, *5*, 1269–1271. (i) Danopoulos, A. A.; Wilkinson, G.; Hussain-Bates, B.; Hursthouse, M. B. *J. Chem. Soc., Dalton Trans.* **1991**, 269–275. (j) McGilligan, B. S.; Arnold, J.; Wilkinson, G.; Hussain-Bates, B.; Hursthouse, M. B. *J. Chem. Soc., Dalton Trans.* **1990**, 2465–2475. (k) Anhaus, J. T.; Kee, T. P.; Schofield, M. H.; Schrock, R. R. *J. Am. Chem. Soc.* **1990**, *112*, 1642–1643. (l) Smieja, J. A.; Shirzad, K.; Roy, M.; Kittilstved, K.; Twamley, B. *Inorg. Chim. Acta* **2002**, *335*, 141–146. (m) Li, Z.-Y.; Huang, J.-S.; Chan, M. C.-W.; Cheung, K.-K.; Che, C.-M. *Inorg. Chem.* **1997**, *36*, 3064–3071. (n) Smieja, J. A.; Omberg, K. M.; Breneman, G. L. *Inorg. Chem.* **1994**, *33*, 614–616. (o) Danopoulos, A. A.; Wilkinson, G.; Hussain-Bates, B.; Hursthouse, M. B. *J. Chem. Soc., Dalton Trans.* **1991**, 1855–1860. (p) Schofield, M. H.; Kee, T. P.; Anhaus, J. T.; Schrock, R. R.; Johnson, K. H.; Davis, W. M. *Inorg. Chem.* **1991**, *30*, 3595–3604. (q) Sellmann, D.; Wemple, M. W.; Donaubauer, W.; Heinemann, F. W. *Inorg. Chem.* **1997**, *36*, 1397–1402. (r) Muñiz, K.; Iesato, A.; Nieger, M. *Chem.—Eur. J.* **2003**, *9*, 5581–5596. (s) LaPointe, A. M.; Schrock, R. R.; Davis, W. M. *Organometallics* **1995**, *14*, 2699–2703.

(25) Cobalt−imido complexes: (a) Jenkins, D. M.; Betley, T. A.; Peters, J. C. *J. Am. Chem. Soc.* **2002**, *124*, 11238–11239. (b) Hu, X.; Meyer, K. *J. Am. Chem. Soc.* **2004**, *126*, 16322–16323. (c) Dai, X.; Kapoor, P.; Warren, T. H. *J. Am. Chem. Soc.* **2004**, *126*, 4798–4799. (d) Shay, D. T.; Yap, G. P. A.; Zakharov, L. N.; Rheingold, A. L.; Theopold, K. H. *Angew. Chem., Int. Ed.* **2005**, *44*, 1508–1510. (e) Cowley, R. E.; Bontchev, R. P.; Sorrell, J.; Sarracino, O.; Feng, Y.; Wang, H.; Smith, J. M. *J. Am. Chem. Soc.* **2007**, *129*, 2424–2425. (f) Jones, C.; Schulten, C.; Rose, R. P.; Stasch, A.; Aldridge, S.; Woodul, W. D.; Murray, K. S.; Moubaraki, B.; Brynda, M.; La Macchia, G.; Gagliardi, L. *Angew. Chem., Int. Ed.* **2009**, *48*, 7406–7410.

(26) Iridium−imido complexes: (a) Glueck, D. S.; Hollander, F. J.; Bergman, R. G. *J. Am. Chem. Soc.* **1989**, *111*, 2719–2721. (b) Glueck, D. S.; Wu, J.; Hollander, F. J.; Bergman, R. G. *J. Am. Chem. Soc.* **1991**, *113*, 2041–2054.

(27) Nickel−imido complexes: (a) Mindiola, D. J.; Hillhouse, G. L. *J. Am. Chem. Soc.* **2001**, *123*, 4623–4624. (b) Waterman, R.; Hillhouse, G. L. *J. Am. Chem. Soc.* **2008**, *130*, 12628–12629. (c) Kogut, E.; Wiencko, H. L.; Zhang, L.; Cordeau, D. E.; Warren, T. H. *J. Am. Chem. Soc.* **2005**, *127*, 11248–11249. (d) Iluc, V. M.; Hillhouse, G. L. *J. Am. Chem. Soc.* **2010**, *132*, 15148–15150. (e) Laskowski, C. A.; Miller, A. J. M.; Hillhouse, G. L.; Cundari, T. R. *J. Am. Chem. Soc.* **2011**, *133*, 771–773.

(28) Jensen, M. P.; Mehn, M. P.; Que, L. *Angew. Chem., Int. Ed.* **2003**, *42*, 4357–4360.

(29) Badiei, Y. M.; Dinescu, A.; Dai, X.; Palomino, R. M.; Heinemann, F. W.; Cundari, T. R.; Warren, T. H. *Angew. Chem., Int. Ed.* **2008**, *47*, 9961–9964.

(30) Thyagarajan, S.; Shay, D. T.; Incarvito, C. D.; Rheingold, A. L.; Theopold, K. H. *J. Am. Chem. Soc.* **2003**, *125*, 4440–4441.

(31) Lucas, R. L.; Powell, D. R.; Borovik, A. S. *J. Am. Chem. Soc.* **2005**, *127*, 11596–11597.

(32) Chomitz, W. A.; Arnold, J. *Chem. Commun.* **2008**, 3648–3650.

(33) King, E. R.; Betley, T. A. *Inorg. Chem.* **2009**, *48*, 2361–2363.

(34) Mankad, N. P.; Müller, P.; Peters, J. C. *J. Am. Chem. Soc.* **2010**, *132*, 4083–4085.

(35) Avenier, F.; Gouré, E.; Dubourdeaux, P.; Sénèque, O.; Oddou, J.-L.; Pécaut, J.; Chardon-Noblat, S.; Deronzier, A.; Latour, J.-M. *Angew. Chem., Int. Ed.* **2008**, *47*, 715–717.

(36) Bai, G.; Stephan, D. W. *Angew. Chem., Int. Ed.* **2007**, *46*, 1856–1859.

(37) Eckert, N. A.; Vaddadi, S.; Stoian, S.; Lachicotte, R. J.; Cundari, T. R.; Holland, P. L. *Angew. Chem., Int. Ed.* **2006**, *45*, 6868–6871.

(38) Cowley, R. E.; DeYonker, N. J.; Eckert, N. A.; Cundari, T. R.; DeBeer, S.; Bill, E.; Ottenwaelder, X.; Flaschenriem, C. J.; Holland, P. L. *Inorg. Chem.* **2010**, *49*, 6172–6187.

(39) HAT reactions by imidomanganese species have been studied and, interestingly, show that the Mn═NR group does not do the HAT reaction itself. See: Zdilla, M. J.; Abu-Omar, M. M. *Inorg. Chem.* **2008**, *47*, 10718–10722.

(40) (a) *Iron Catalysis in Organic Chemistry: Reactions and Applications*; Plietker, B., Ed.; Wiley-VCH: Weinheim, Germany, 2008. (b) Bolm, C.; Legros, J.; Le Paih, J.; Zani, L. *Chem. Rev.* **2004**, *104*, 6217–6254. (c) Fürstner, A. *Angew. Chem., Int. Ed.* **2009**, *48*, 1364–1367.

(d) Correa, A.; Mancheño, O. G.; Bolm, C. *Chem. Soc. Rev.* **2008**, *37*, 1108–1117. (e) Bauer, E. B. *Curr. Org. Chem.* **2008**, *12*, 1341–1369.

(41) Chiang, K. P.; Barrett, P. M.; Ding, F.; Smith, J. M.; Kingsley, S.; Brennessel, W. W.; Clark, M. M.; Lachicotte, R. J.; Holland, P. L. *Inorg. Chem.* **2009**, *48*, 5106–5116.

(42) Cobaltocene is a convenient integration standard for our paramagnetic ^{1}H NMR spectra since it gives a single intense resonance (δ −51 ppm at 25 °C in C_6D_6) with a similar line width to the resonances of our compounds.

(43) *KaleidaGraph 3.51*; Synergy Software, 2000.

(44) We used the values for the Hammett constant σ_p given in Table 1 of Hansch, C.; Leo, A.; Taft, R. W. *Chem. Rev.* **1991**, *91*, 165–195.

(45) Luo, Y.-R. *Comprehensive Handbook of Chemical Bond Energies*; CRC Press: Boca Raton, FL, 2007.

(46) Gao, Y.; DeYonker, N. J.; Garrett, E. C.; Wilson, A. K.; Cundari, T. R.; Marshall, P. *J. Phys. Chem. A* **2009**, *113*, 6955–6963.

(47) We also investigated the postreaction mixture in the reaction between **1**·^{t}**Bupy** and indene. A small quantity (<5%) of 1,1′-biindene was detected, but the ultimate fate of the putative indenyl radical is unclear.

(48) Rappé, A. K.; Casewit, C. J.; Colwell, K. S.; Goddard, W. A.; Skiff, W. M. *J. Am. Chem. Soc.* **1992**, *114*, 10024–10035.

(49) Conradie, J.; Ghosh, A. *J. Chem. Theory Comput.* **2007**, *3*, 689–702.

(50) X-band EPR spectra at 10 K of various mixtures of **1** and ^{t}Bupy show only an $S = 3/2$ signal as previously reported (ref 37), with no sign of an $S = 5/2$ signal. The solution magnetic moment of a solution of **1** + 0.5 M ^{t}Bupy was $\mu_{eff} = 4.0(2)$ BM, also supporting an $S = 3/2$ ground state of **1**·^{t}**Bupy**.

(51) Geometry-optimized **1**·^{t}**Bupy** has τ_4 values of 0.73 (sextet) and 0.94 (quartet). The calculated τ_4 parameter is 0.85 for an ideal trigonal pyramid and 1.00 for an ideal tetrahedron. See: Yang, L.; Powell, D. R.; Houser, R. P. *Dalton Trans.* **2007**, 955–964.

(52) Eckert, N. A.; Smith, J. M.; Lachicotte, R. J.; Holland, P. L. *Inorg. Chem.* **2004**, *43*, 3306–3321.

(53) Bordwell, F. G.; Cheng, J.-P.; Satish, A. V.; Twyman, C. L. *J. Org. Chem.* **1992**, *57*, 6542–6546.

(54) Rüchardt, C.; Gerst, M.; Ebenhoch, J. *Angew. Chem., Int. Ed. Engl.* **1997**, *36*, 1406–1430.

(55) Compiled BDE data often list a range of BDE values for the same compound. For example, ref 45 gives five different values for the BDE of the benzylic C−H bond in ethylbenzene, which range from 84.6 to 90.3 kcal/mol.

(56) Bordwell, F. G.; Drucker, G. E. *J. Org. Chem.* **1980**, *45*, 3325–3328.

(57) Alnajjar, M. S.; Zhang, X.-M.; Gleicher, G. J.; Truksa, S. V.; Franz, J. A. *J. Org. Chem.* **2002**, *67*, 9016–9022.

(58) Rosenstock, H. M.; Draxl, K.; Steiner, B. W.; Herron, J. T. In *NIST Chemistry WebBook, NIST Standard Reference Database Number 69*; Linstrom, P. J., Mallard, W. G., Eds.; National Institute of Standards and Technology: Gaithersburg, MD. http://webbook.nist.gov (accessed March 9, 2011).

(59) Lee, R. E.; Squires, R. R. *J. Am. Chem. Soc.* **1986**, *108*, 5078–5086.

(60) Note that the relative gas-phase enthalpies of formation of 1,3- and 1,4-cyclohexadiene are essentially identical (25.00 ± 0.15 kcal/mol and 24−26 kcal/mol, respectively).

(61) Meot-Ner, M.; Liebman, J. F.; Kafafi, S. A. *J. Am. Chem. Soc.* **1988**, *110*, 5937–5941.

(62) Taft, R. W.; Bordwell, F. G. *Acc. Chem. Res.* **1988**, *21*, 463–469.

(63) (a) Wiberg, K. B. *Chem. Rev.* **1955**, *55*, 713–743. (b) Westheimer, F. H. *Chem. Rev.* **1961**, *61*, 265–273.

(64) (a) Ingold, K. U. In *Hydrogen-Transfer Reactions*; Hynes, J. T., Klinman, J. P., Limbach, H.-H., Schowen, R. L., Eds.; Wiley-VCH: Weinheim, Germany, 2007; Vol. 2, pp 875−894. (b) Knapp, M. J.; Meyer, M.; Klinman, J. P. In *Hydrogen-Transfer Reactions*; Hynes, J. T., Klinman, J. P., Limbach, H.-H., Schowen, R. L., Eds.; Wiley-VCH: Weinheim, Germany, 2007; Vol. 4, pp 1241−1284.

(65) Huynh, M. H. V.; Meyer, T. J. *Chem. Rev.* **2007**, *107*, 5004–5064.

(66) Binstead, R. A.; McGuire, M. E.; Dovletoglou, A.; Seok, W. K.; Roecker, L. E.; Meyer, T. J. *J. Am. Chem. Soc.* **1992**, *114*, 173–186.

(67) Huynh, M. H. V.; Meyer, T. J. *Proc. Natl. Acad. Sci. U.S.A.* **2004**, *101*, 13138–13141.

(68) (a) Ingold, K. U. *Acc. Chem. Res.* **1969**, *2*, 1–9. (b) Howard, J. A.; Ingold, K. U. *Can. J. Chem.* **1963**, *41*, 1744–1751. (c) Howard, J. A.; Ingold, K. U. *Can. J. Chem.* **1963**, *41*, 2800–2806. (d) Brownlie, I. T.; Ingold, K. U. *Can. J. Chem.* **1966**, *44*, 861–868. (e) Middleton, B. S.; Ingold, K. U. *Can. J. Chem.* **1967**, *45*, 191–194.

(69) For example: (a) Mayer, J. M. *Acc. Chem. Res.* **1998**, *31*, 441–450. (b) Bryant, J. R.; Mayer, J. M. *J. Am. Chem. Soc.* **2003**, *125*, 10351–10361. (c) Miyazaki, S.; Kojima, T.; Mayer, J. M.; Fukuzumi, S. *J. Am. Chem. Soc.* **2009**, *131*, 11615–11624. (d) Gardner, K. A.; Mayer, J. M. *Science* **1995**, *269*, 1849–1851. (e) Larsen, A. S.; Wang, K.; Lockwood, M. A.; Rice, G. L.; Won, T.-J.; Lovell, S.; Sadílek, M.; Tureček, F.; Mayer, J. M. *J. Am. Chem. Soc.* **2002**, *124*, 10112–10123. (f) Roth, J. P.; Mayer, J. M. *Inorg. Chem.* **1999**, *38*, 2760–2761.

(70) Yiu, D. T. Y.; Lee, M. F. W.; Lam, W. W. Y.; Lau, T.-C. *Inorg. Chem.* **2003**, *42*, 1225–1232.

(71) (a) Lucarini, M.; Pedrielli, P.; Pedulli, G. F. *J. Org. Chem.* **1996**, *61*, 9259–9263. (b) Burton, G. W.; Doba, T.; Gabe, E. J.; Hughes, L.; Lee, F. L.; Prasad, L.; Ingold, K. U. *J. Am. Chem. Soc.* **1985**, *107*, 7053–7065. (c) Franchi, P.; Lucarini, M.; Pedulli, G. F.; Valgimigli, L.; Lunelli, B. *J. Am. Chem. Soc.* **1999**, *121*, 507–514.

(72) Man, W.-L.; Lam, W. W. Y.; Kwong, H.-K.; Peng, S.-M.; Wong, W.-T.; Lau, T.-C. *Inorg. Chem.* **2010**, *49*, 73–81.

(73) Mukherjee, A.; Martinho, M.; Bominaar, E. L.; Münck, E.; Que, L. *Angew. Chem., Int. Ed.* **2009**, *48*, 1780–1783.

(74) Newhouse, T.; Baran, P. S. *Angew. Chem., Int. Ed.* **2011**, *50*, 3362–3374.

(75) Mayer, J. M. *Acc. Chem. Res.* **2011**, *44*, 36–46.

(76) Zdilla, M. J.; Dexheimer, J. L.; Abu-Omar, M. M. *J. Am. Chem. Soc.* **2008**, *129*, 11505–11511.

(77) Man, W.-L.; Lam, W. W. Y.; Yiu, S.-M.; Lau, T.-C.; Peng, S.-M. *J. Am. Chem. Soc.* **2004**, *126*, 15336–15337.

(78) Venkataramanan, N. S.; Rajagopal, S. *Tetrahedron* **2006**, *62*, 5645–5651.

(79) Prokop, K. A.; de Visser, S. P.; Goldberg, D. P. *Angew. Chem., Int. Ed.* **2010**, *49*, 5091–5095.

(80) (a) Green, M. T.; Dawson, J. H.; Gray, H. B. *Science* **2004**, *304*, 1653–1656. (b) Behan, R. K.; Hoffart, L. M.; Stone, K. L.; Krebs, C.; Green, M. T. *J. Am. Chem. Soc.* **2006**, *128*, 11471–11474. (c) Dey, A.; Jiang, Y.; Ortiz de Montellano, P.; Hodgson, K. O.; Hedman, B.; Solomon, E. I. *J. Am. Chem. Soc.* **2009**, *131*, 7869–7878.

(81) Isborn, C.; Hrovat, D. A.; Borden, W. T.; Mayer, J. M.; Carpenter, B. K. *J. Am. Chem. Soc.* **2005**, *127*, 5794–5795.

(82) Cundari, T. R.; Russo, M. *J. Chem. Inf. Comput. Sci.* **2001**, *41*, 281–287.

(83) (a) Shaik, S.; Hirao, H.; Kumar, D. *Acc. Chem. Res.* **2007**, *40*, 532–542. (b) Hirao, H.; Que, L.; Nam, W.; Shaik, S. *Chem.—Eur. J.* **2008**, *14*, 1740–1756. (c) Bassan, A.; Blomberg, M. R. A.; Siegbahn, P. E. M.; Que, L. *Chem.—Eur. J.* **2005**, *11*, 692–705. (d) Kumar, D.; Hirao, H.; Que, L.; Shaik, S. *J. Am. Chem. Soc.* **2005**, *127*, 8026–8027.

(84) (a) Que, L. *Acc. Chem. Res.* **2007**, *40*, 493–500. (b) Nam, W. *Acc. Chem. Res.* **2007**, *40*, 522–531. (c) Rohde, J.-U.; Que, L. *Angew. Chem.* **2005**, *44*, 2255–2258. (d) Rohde, J.-U.; In, J.-H.; Lim, M. H.; Brennessel, W. W.; Bukowski, M. R.; Stubna, A.; Münck, E.; Nam, W.; Que, L. *Science* **2003**, *299*, 1037–1039. (e) Lim, M. H.; Rohde, J.-U.; Stubna, A.; Bukowski, M. R.; Costas, M.; Ho, R. Y. N.; Münck, E.; Nam, W.; Que, L. *Proc. Natl. Acad. Sci. U.S.A.* **2003**, *100*, 3665–3670. (f) Jensen, M. P.; Costas, M.; Ho, R. Y. N.; Kaizer, J.; Payeras, A. M.; Münck, E.; Que, L.; Rohde, J.-U.; Stubna, A. *J. Am. Chem. Soc.* **2005**, *127*, 10512–10525. (g) Zhou, Y.; Shan, X.; Mas-Balleste, R.; Bukowski, M. R.; Stubna, A.; Chakrabarti, M.; Slominski, L.; Halfen, J. A.; Münck, E.; Que, L. *Angew. Chem., Int. Ed.* **2008**, *47*, 1896–1899. (h) Li, F.;

England, J.; Que, L. *J. Am. Chem. Soc.* **2010**, *132*, 2134–2135. (i) Decker, A.; Rohde, J.-U.; Que, L.; Solomon, S. I. *J. Am. Chem. Soc.* **2004**, *126*, 5378–5379. (j) England, J.; Guo, Y.; Farquhar, E. R.; Young, V. G.; Münck, E.; Que, L. *J. Am. Chem. Soc.* **2010**, *132*, 8635–8644.

(85) An Fe^{IV}═O complex with an $S = 2$ ground state has recently been described; see refs 12h and 84j.

(86) Hammond, G. S. *J. Am. Chem. Soc.* **1955**, *77*, 334–338.

(87) The same trend in basicity causes polar C−H activation by addition to M−N single bonds to be faster than that for analogous M−O single bonds. See: Cundari, T. R.; Grimes, T. V.; Gunnoe, T. B. *J. Am. Chem. Soc.* **2007**, *129*, 13172–13182.

(88) Meot-Ner, M. *J. Am. Chem. Soc.* **1982**, *104*, 5–10.

(89) Gbara-Haj-Yahia, I.; Zvilichovsky, G.; Seri, N. *J. Org. Chem.* **2004**, *69*, 4135–4139.

(90) Paquette, L. A.; Kakihana, T.; Hansen, J. F.; Philips, J. C. *J. Am. Chem. Soc.* **1971**, *93*, 152–161.

(91) (a) Ammann, C.; Meier, P.; Merbach, A. E. *J. Magn. Reson.* **1982**, *46*, 319–321. (b) Kaplan, M. L.; Bovey, F. A.; Cheng, H. N. *Anal. Chem.* **1975**, *47*, 1703–1705.

(92) Goldsmith, C. R.; Jonas, R. T.; Stack, T. D. P. *J. Am. Chem. Soc.* **2002**, *124*, 83–96.

(93) Yasuda, M.; Pac, C.; Sakurai, H. *Bull. Chem. Soc. Jpn.* **1980**, *53*, 502–507.

(94) Frisch, M. J.; et al. *Gaussian 09*; Gaussian Inc.: Pittsburgh, PA, 1998. The full author list may be found in the Supporting Information.

(95) (a) Becke, A. D. *Phys. Rev.* **1998**, *A38*, 3098–3100. (b) Becke, A. D. *J. Chem. Phys.* **1993**, *98*, 1372–1377. (c) Becke, A. D. *J. Chem. Phys.* **1993**, *98*, 5648–5652. (d) Lee, C.; Yang, W.; Parr, R. G. *Phys. Rev.* **1988**, *B37*, 785–789.

(96) Svensson, M.; Humbel, S.; Froese, R. D. J.; Matsubara, T.; Sieber, S.; Morokuma, K. *J. Phys. Chem.* **1996**, *100*, 19357–19363.

(97) (a) Casewit, C. J.; Colwell, K. S.; Rappé, A. K. *J. Am. Chem. Soc.* **1992**, *114*, 10035–10046. (b) Rappé, A. K.; Casewit, C. J.; Colwell, K. S.; Goddard, W. A.; Skiff, W. M. *J. Am. Chem. Soc.* **1992**, *114*, 10024–10035.